

AFRL-VA-WP-TR-2003-3012

FRETTING FATIGUE MODEL

**C.L. Brooks
S.A. Prost-Domasky
K.T. Honeycutt
T.B. Mills
N. Young**

**APES, Inc.
6669 Fyler Avenue
St. Louis, MO 63139**



FEBRUARY 2003

Final Report for 01 February 2002 – 30 November 2002

THIS IS A SMALL BUSINESS INNOVATION RESEARCH (SBIR) PHASE I REPORT

Approved for public release; distribution is unlimited.

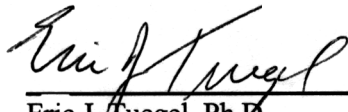
**AIR VEHICLES DIRECTORATE
AIR FORCE MATERIEL COMMAND
AIR FORCE RESEARCH LABORATORY
WRIGHT-PATTERSON AIR FORCE BASE, OH 45433-7542**

NOTICE

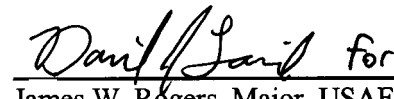
USING GOVERNMENT DRAWINGS, SPECIFICATIONS, OR OTHER DATA INCLUDED IN THIS DOCUMENT FOR ANY PURPOSE OTHER THAN GOVERNMENT PROCUREMENT DOES NOT IN ANY WAY OBLIGATE THE US GOVERNMENT. THE FACT THAT THE GOVERNMENT FORMULATED OR SUPPLIED THE DRAWINGS, SPECIFICATIONS, OR OTHER DATA DOES NOT LICENSE THE HOLDER OR ANY OTHER PERSON OR CORPORATION; OR CONVEY ANY RIGHTS OR PERMISSION TO MANUFACTURE, USE, OR SELL ANY PATENTED INVENTION THAT MAY RELATE TO THEM.

THIS REPORT IS RELEASABLE TO THE NATIONAL TECHNICAL INFORMATION SERVICE (NTIS). AT NTIS, IT WILL BE AVAILABLE TO THE GENERAL PUBLIC, INCLUDING FOREIGN NATIONS.


THIS TECHNICAL REPORT HAS BEEN REVIEWED AND IS APPROVED FOR PUBLICATION.



Eric J. Tuegel, Ph.D.
Engineer
Aircraft Structural Integrity



James W. Rogers, Major, USAF
Chief
Analytical Structural Mechanics Branch



Jeffrey S. Turcotte, Lt. Col., USAF
Chief
Structures Division

Do not return copies of this report unless contractual obligations or notice on a specific document require its return.

REPORT DOCUMENTATION PAGE					<i>Form Approved</i> <i>OMB No. 0704-0188</i>	
The public reporting burden for this collection of information is estimated to average 1 hour per response, including the time for reviewing instructions, searching existing data sources, gathering and maintaining the data needed, and completing and reviewing the collection of information. Send comments regarding this burden estimate or any other aspect of this collection of information, including suggestions for reducing this burden, to Department of Defense, Washington Headquarters Services, Directorate for Information Operations and Reports (0704-0188), 1215 Jefferson Davis Highway, Suite 1204, Arlington, VA 22202-4302. Respondents should be aware that notwithstanding any other provision of law, no person shall be subject to any penalty for failing to comply with a collection of information if it does not display a currently valid OMB control number. PLEASE DO NOT RETURN YOUR FORM TO THE ABOVE ADDRESS.						
1. REPORT DATE (DD-MM-YY) February 2003		2. REPORT TYPE Final		3. DATES COVERED (From - To) 02/01/2002 – 11/30/2002		
4. TITLE AND SUBTITLE FRETTING FATIGUE MODEL				5a. CONTRACT NUMBER F33615-02-M-3204		
				5b. GRANT NUMBER		
				5c. PROGRAM ELEMENT NUMBER 65502D		
6. AUTHOR(S) C.L. Brooks S.A. Prost-Domasky K.T. Honeycutt T.B. Mills N. Young				5d. PROJECT NUMBER 3005		
				5e. TASK NUMBER 42		
				5f. WORK UNIT NUMBER 2F		
7. PERFORMING ORGANIZATION NAME(S) AND ADDRESS(ES) APES, Inc. 6669 Fyler Avenue St. Louis, MO 63139				8. PERFORMING ORGANIZATION REPORT NUMBER		
9. SPONSORING/MONITORING AGENCY NAME(S) AND ADDRESS(ES) Air Vehicles Directorate Air Force Research Laboratory Air Force Materiel Command Wright-Patterson AFB, OH 45433-7542				10. SPONSORING/MONITORING AGENCY ACRONYM(S) AFRL/VASM		
				11. SPONSORING/MONITORING AGENCY REPORT NUMBER(S) AFRL-VA-WP-TR-2003-3012		
12. DISTRIBUTION/AVAILABILITY STATEMENT Approved for public release; distribution is unlimited.						
13. SUPPLEMENTARY NOTES This is a Small Business Innovation Research (SBIR) Phase I report. Report contains color.						
14. ABSTRACT <p>The multitask objectives of the plan discussed in this proposal are to research the role and effects of fretting on structural life of components; develop and demonstrate the feasibility of integrating candidate fretting fatigue predictive analytic model(s) into structural integrity methods; integrate and implement the techniques for applications to present and future U.S. military weapons programs, commercial aviation, automotive, and mechanical equipment; and provide industry access to the predictive tools and information for commercialization.</p>						
15. SUBJECT TERMS corrosion-fatigue, fretting fatigue, damage tolerance, structural integrity, life assessments, life predictions, damage simulations						
16. SECURITY CLASSIFICATION OF:			17. LIMITATION OF ABSTRACT: SAR	18. NUMBER OF PAGES 58	19a. NAME OF RESPONSIBLE PERSON (Monitor) Dr. Eric Tuegel 19b. TELEPHONE NUMBER (Include Area Code) (937) 904-6772	
a. REPORT Unclassified	b. ABSTRACT Unclassified	c. THIS PAGE Unclassified				

TABLE OF CONTENTS

<u>Section</u>	<u>Page</u>
LIST OF FIGURES	iv
LIST OF TABLES	vi
SUMMARY	1
1.0 INTRODUCTION	2
1.1 Background	2
1.2 Holistic Life Prediction Methodology (HLPM).....	3
2.0 PHASE I TASKS	6
2.1 Task I: Research Current Approaches	6
2.1.1 Early Experimental and Analytical Research	6
2.1.2 Recently Developed Analytical Approaches	8
2.1.3 Non-destructive Testing (NDT)	8
2.1.4 Fretting Maps	9
2.2 Task II: Fretting Fatigue Candidate Model Development	12
2.2.1 Hattori Model.....	12
2.2.2 Crack Analogue Model	16
2.3 Task III: Development of Fretting Fatigue Test Plan	19
2.3.1 Non-destructive Detection of Fretting	21
2.3.1.1 Conventional Non-destructive Testing	20
2.3.1.2 Fuji Film Tests	20
2.3.1.3 NDT Tests in Lap Joints	25
2.3.2 Fretting Fatigue Test Program	25
2.3.2.1 IDS Characterization (Baseline Fatigue)	27
2.3.2.2 Fretting Fatigue Behavior in Low K_t Coupons	28
2.3.2.3 Fretting Fatigue Behavior in High K_t Coupons	31
2.3.2.4 Single Rivet Lap Joint (SLRJ) Fatigue Tests	32
2.3.2.5 Multiple Rivet Lap Joint (MRLJ) Fatigue Tests	33
2.4 Task IV: Fretting Fatigue Model Integration.....	34
2.4.1 Correlation	35
2.4.2 Validation of Rooke and Jones Methods	38
2.4.3 Validation of Normal Contact Pressure Simulations	39
2.4.4 Single Rivet Lap Joint (SRLJ) Simulations	39
3.0 CONCLUSIONS.....	42
4.0 REFERENCES	43
LIST OF ACRONYMS	48

LIST OF FIGURES

<u>Figure</u>	<u>Page</u>
1. Robust Structural Life Prediction Methodology Accommodates Fretting Fatigue Methodology. Points of Emphasis in Fretting are Cracking Scenarios (Modes and Patterns, Sizes and Shapes), Crack Driving Forces (Microstresses), and Load Spectra (Dynamic).	5
2. Holistic Approach Accounts for All Known Effects and Will Determine All States of Damage from Stage I (As-Manufactured) through Stage IV (Too Late).....	5
3. Fretting Fatigue Methodology	7
4. Shear and Displacements Measurements Allow Separation of Fretting Modes. Stick Mode Characterized by Elastic Deformations, Little Plastic Strain or Hysteresis. Stick-Slip Mode Characterized by Some Hysteresis. Full or Gross Slip Characterized by Large Hysteresis Loops. Vingsbo (61).	10
5. Material Response Fretting Map (MRFM). Vincent (35).....	10
6. Running Condition Fretting Map (RCFM). Vincent (35).....	11
7. Fracture Mechanics Method Uses the Rooke and Jones Stress Intensity Factor Solution for Point Loads Effects	13
8. Fracture Mechanics Method Extends the Rooke and Jones Stress Intensity Factor Solution to Spatially Varying Amplitude Normal and Shear Traction	13
9. Fracture Mechanics Method Models the Fretting Pad with Normal and Shear Contact on Fatigued Coupon.....	15
10. ‘Crack Analogue’ Model Uses the Asymptotic Stress Field as the Poker Corner is Approached in the Substrate	16
11. ‘Crack Analogue’ Model Uses the Asymptotic Stress Field at the Crack Tip in a Double-Edge Crack in Semi-infinite Body Loaded by Point Normal and Shear Loads at Infinity.....	16
12. ‘Crack Analogue’ Cracking Scenario Consists of Constant Inclination Crack Originating at Crack Tip that ‘Kinks’ or Turns When the Stress Intensity Factor Due to the Far Field Stress is Larger than the ‘Local’ Stress Intensity Factor at Inclined Crack Tip.....	18
13. Fuji Pressure Sensitive Film Is Two-Part Medium.	21

LIST OF FIGURES (continued)

<u>Figure</u>	<u>Page</u>
14. SRLJ Specimen Top View.....	22
15. SRLJ Side View. Note Pressure Sensitive Film Sandwiched Between Both Layers (arrows).....	22
16. Individual Results - High, Medium and Low Film (Left to Right).....	23
17. Sandwich results – High, Medium, and Low Film (Left to Right).....	23
18. Fifteen-Rivet Lap Joint (MRLJ) to Be Tested.	24
19. Building Block Approach Requires Validation of Analytical Methods with Simple Coupon Tests first, Then Element/Geometric Tests, etc.	26
20. Hole Configuration to Be Tested. Two Geometries of Fretting Pads Will Be Tested, and Will Be Similar to Those Shown Schematically.	31
21. Flat Punch Model in ECLIPSE Implements Hattori’s Model and Can be Easily Extended to Incorporate ‘Crack Analogue’.	35
22. Time-Dependent Fretting Inputs to ECLIPSE.	36
23. ECLIPSE Output Including Fretting Contribution to Holistic Analysis.....	37
24. Hattori Closed-Form Fretting Model Behavior, Material Model A.....	40
25. Hattori Closed-Form Fretting Model Behavior, Material Model B.....	40
26. StressCheck Finite Element Mesh Used to Simulate Flat Pad Contact..	41

LIST OF TABLES

<u>Table</u>	<u>Page</u>
1. Pressure Ranges for Pressure Sensitive Film.....	22
2. Proposed Test Matrix	27
3. Test Matrix for Baseline Fatigue Behavior.....	27
4. Bench Test matrix for Low Kt fretting fatigue	28
5. Test Matrix for Low Kt Fretting Fatigue	30
6. High Kt Test Matrix for Fretting Fatigue.....	32
7. Test Matrix for Single Rivet Lap Joint Experiments	33

SUMMARY

Fretting is a wear phenomenon that occurs between two mating surfaces. It is adhesive in nature, and vibration is its essential causative factor. Frequently fretting is accompanied by corrosion. In general, fretting occurs between two tight fitting surfaces that are subjected to a cyclic, relative motion of extremely small amplitude. Fretted regions are highly sensitive to fatigue cracking. Under fretting conditions fatigue cracks are nucleated at very low loads. Nucleation of fatigue cracks in fretted regions depends mainly on the state of stress on the surface and particularly on the stresses superimposed on the cyclic stress. The time to nucleation of cracks can be significantly reduced as a result of fretting. Common sites for fretting are in joints that are bolted, keyed, pinned, press fitted, and riveted. These sites are common in the assembly of most air vehicles, ground vehicles, power plants, equipment, and machinery. All applications that have safety issues, maintenance issues, and service life requirements will benefit from quantitative methods that provide the impact of fretting on the component's service.

The following objectives of this Phase I SBIR project were accomplished:

- 1) An extensive literature search was conducted to investigate past and current methods, data, approaches, and experience for modeling fretting influences on mechanical fatigue in structure,
- 2) The two candidate fretting fatigue analytical approaches were identified,
- 3) One fretting fatigue predictive analytic model was integrated into an existing structural integrity framework to demonstrate feasibility of our approach,
- 4) An experimental test plan to implement and verify the analytical fretting models was developed,
- 5) An implementation and integration program that results in a viable commercialization strategy was prepared and described.

Research and development efforts in Phase I indicated that the enabling technologies are mature enough to allow introduction of fretting fatigue into a life prediction methodology; analytical predictive models have been developed and validated against simple coupon data. NDT techniques, though based on relatively new technologies, are mature enough to provide some indications of fretting and fretting damage. The Phase I effort has shown the feasibility of incorporating these technologies, although there is more research needed to ensure the models become robust.

1.0 INTRODUCTION

1.1 Background

Condition-based maintenance (CBM) is maintenance action based on the actual condition obtained from in-situ, non-invasive tests, operating and condition measurements (1). CBM has the potential to improve safety and readiness, and reduce by 30% operation & support costs, which accounts for about 65% of total life-cycle costs by (1):

- assuring optimum efficiency,
- minimizing failures; threats to safety, direct and collateral damage to equipment,
- safely reducing or eliminating Planned Maintenance,
- identifying chronic defects, individual and class,
- providing guidelines for new equipment purchase,
- effectively prioritizing decreasing resources

Reliable CBM requires a robust method or tool to assess the severity of damage that is detected and estimate how fast it will grow in order to plan for maintenance; that is, an analytical model that integrates all damage mechanisms such as corrosion, fatigue and fretting. Corrosion and fatigue have already been incorporated into and demonstrated with an existing life prediction framework (the Holistic Life Prediction Methodology—HLPM—described in the next Section); the HLPM has thus far seems to be a viable life prediction approach, incorporating time and cycle dependence. In addition, the HLPM has the flexibility to integrate damage models that account for fretting and fretting fatigue effects.

What is fretting? Fretting is a wear phenomenon that occurs between two mating surfaces: it is adhesive in nature, and vibration is its essential causative factor. Frequently fretting is accompanied by corrosion. In general, fretting occurs between two tight fitting surfaces that are subjected to a cyclic, relative motion of extremely small amplitude. Fretted regions are highly sensitive to fatigue cracking. Under fretting conditions fatigue cracks can nucleate in even at stresses in the fretted structure that are lower than the endurance limit, often resulting in structural failure that occurs at many more cycles than anticipated. Nucleation of fatigue cracks in fretted regions depends mainly on the state of stress on the surface and particularly on the stresses superimposed on the cyclic stress. The time to nucleation of cracks can be significantly reduced as a result of fretting. Common sites for fretting are in joints that are bolted, keyed, pinned, press fitted, and riveted. These sites are common in the assembly of most air vehicles, ground vehicles, power plants, equipment, and machinery.

Fretting damage is differentiated by three distinct modes: fretting wear, fretting fatigue, and gross sliding wear. Fretting wear, which occurs for relatively small vibratory motion, normally results in relatively little damage and rarely causes premature structural failure. Gross sliding wear, which occurs for relatively large vibratory motion, normally results in visual surface damage, but rarely causes premature structural failure. Fretting fatigue, caused by intermediate vibratory motion, is the most damaging, causes cracking and often results in premature structural failure. This Phase I SBIR project focused primarily on the structural damage associated with this last mode, that is, fretting fatigue. The HLPM framework was used as the framework for integrating fretting fatigue models. The primary goal of Phase I

was to determine how analytical models for fretting fatigue life prediction can be incorporated into a fracture mechanics-based crack growth code. An added bonus is that APES has been developing corrosion fatigue analysis capability in the HLPM framework, so this effort also investigated the integration of fretting, corrosion and fatigue into a single structural analysis tool.

1.2 Holistic Life Prediction Methodology (HLPM)

Though it is well known that corrosion and other age-degradation effects have detrimental influences on the cyclic behavior of aircraft structures, the role and contribution of fretting is not accounted for and not widely recognized. As noted by the definition of fretting in the Metals Handbook (2), the principal causation of fretting is stress cycles, with corrosion providing an environment catalyst. Recent advances in life prediction methods have evolved that include the effects of operational cycles and time dependent degradation, e.g., corrosion, in life assessment tools. USAF Aircraft Structural Integrity Programs (ASIP) are presently implementing practices that account for these effects, but so far do not include the specific damage contributions from fretting. As previously described by Brooks and Simpson (58), technologies will allow incorporation of corrosion and age-degradation effects, which may include fretting if the geometry of the fretting pad and the fretted structure evolve in time, into a systematic damage tolerance (DT) approach are sufficiently mature that their integration into the current ASIP framework is feasible. The framework is readily adaptable to multiple flight vehicles systems, rail, automotive, and mechanical equipment systems. The life prediction methodology was enhanced in part under Contracts F09603-95-D-0053 and F09603-97-D-0550, sponsored by the USAF Corrosion Program office at Warner-Robins AFB, GA. The ability of the methodology to predict unanticipated field aircraft cracking problems indicates that the techniques (advanced finite element methods with reliable stress intensity factor calculations (24), improved analytical modes that allow inclusion of time domain effects such as pillowing by corrosion by products in lap joints (72), models that use local stress amplifications due to pitting (24) and an analytical framework that is based upon simulation of a structure from the as-manufactured state utilizing damage growth fundamentals (72), for instance) support engineering tools that are in development, allowing the analyst to possess the capability to quantify the effects of age degradation on the structural service life of aircraft structure (73). This has been demonstrated by the correlation of the predicted lives with the measured fatigue lives of controlled corrosion-fatigue experiments completed by the University of Utah and NRC-Canada in the Corrosion Program office funded research (73) The framework and computational techniques of these models can readily incorporate the damage effects of fretting.

A description of the basic model framework is documented in a report by Brooks, et.al. (59). APES are the principal developers of the predictive framework and the associated computer code, ECLIPSE[®] (Environmental Cyclic Life Interaction Prediction SoftwarE). This structural life prediction framework extends concepts of damage accumulation from operational stress excursions of the aircraft to include damage accumulation from elapsed time on the ground and the exposure to differing environments. The model has the flexibility to represent material behavior and include variations in material susceptibility to different environmentally assisted mechanisms in the “crack growth rate domain” during operation.

Also, the model when accounting for age degradation includes material behavior differences and susceptibilities that represent corrosion degradation and corrosion rates with stress assisted mechanisms in the “time domain”. Similarly, the inclusion of fretting damage mechanisms requires understanding the physical conditions and effects in both domains that are associated with the fretting phenomena.

Combining the cyclic and time domains results in a method that can compute the full service life capability, i.e., “the holistic life” that includes all damage-generating processes of structures and systems. The holistic approach requires a method that provides a description of the as-produced, or as-manufactured, condition of the structure to establish the initial analysis condition. The initial analysis condition that describes the physical characteristics and numerical boundary use a concept referred to as the “Initial Discontinuity State” (IDS, sometimes called the “Initial Quality State” (IQS)) concept (60). For analyses that include the age degradation effects, the early stages of cracking become very important. Fretting plays a significant role in these early stages. Selection of flaw shapes and modes of cracking are input parameters used to formulate the type of corrosion degradation to be included in the analysis and the calibration of the IDS concept, which includes the use of ‘physical’ material features, i.e., intrinsic discontinuities such as cracked particles that have size and shape. These features become input parameters that form the starting discontinuity size to be extended by damaging mechanisms, in this case fretting. A holistic approach also accounts for both internal and externally induced states of stress ranging from the micro scale to the macro scale and on to global far-field stresses. All flaw size regimes, especially the short cracks, must be considered. Stress influences on the life prediction for the cyclic portion of the analysis consider the stress excursions from operational flight and ground handling loading. To include age degradation effects into the predictive model, factoring of the incremental effects of time-dependent corrosion degradation mechanisms over into the cyclic regime is required. These degradation effects include all levels of scale in the fracture model, levels that had been neglected when using traditional damage tolerance approaches, Figure 1.

The resulting predictions from the model attempt to compute the quasi-stochastic structural lives that can occur in a component, depending upon the conditions that exist and potential conditions that will be induced due to operational usage and maintenance. The predictions provide intermediate values throughout the entire crack size regime. The holistic process Stage progression is schematically shown on Figure 2.

Current damage tolerance procedures tend to focus on the center two ranges (Stage II and III), whereas the holistic concept attempts to account for and compute age degradation with cyclic stress effects in all four stages. This allows analysts to account for the critical stages when and where they are important, rather than forcing potentially conservative procedures at all locations. The effects of fretting appear to be most important in Stage I, therefore a considerable portion of the experimental test matrix described below will address fretting in the early stages of structural life.

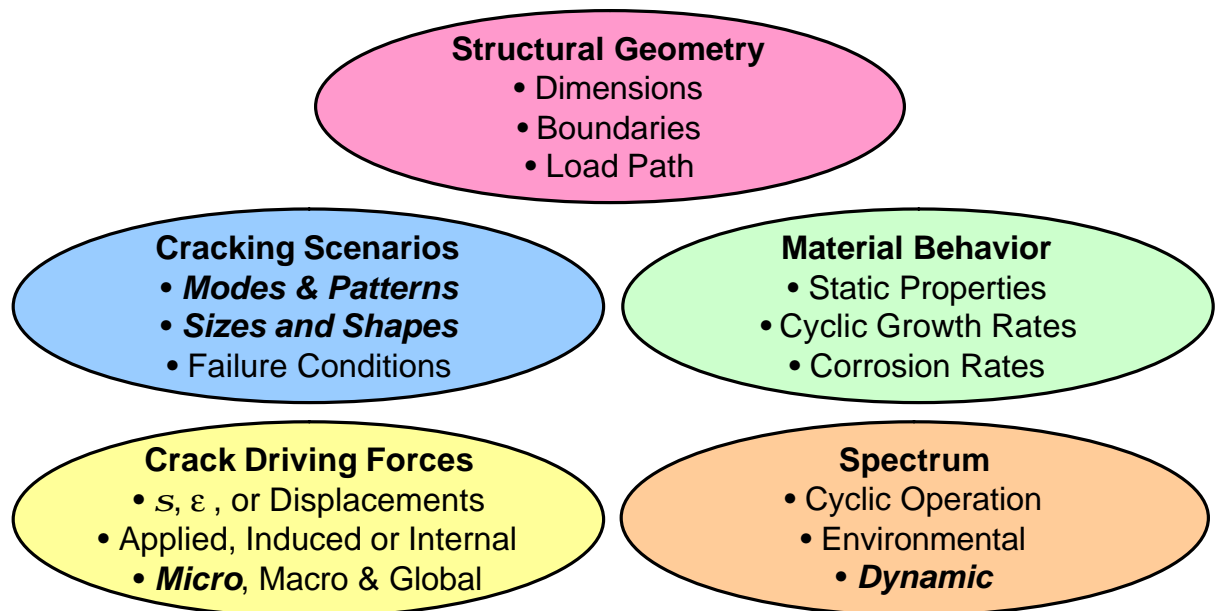


Figure 1 Robust Structural Life Prediction Methodology Accommodates Fretting Fatigue Methodology. Points of Emphasis in Fretting are Cracking Scenarios (Modes and Patterns, Sizes and Shapes), Crack Driving Forces (Microstresses), and Load Spectra (Dynamic).

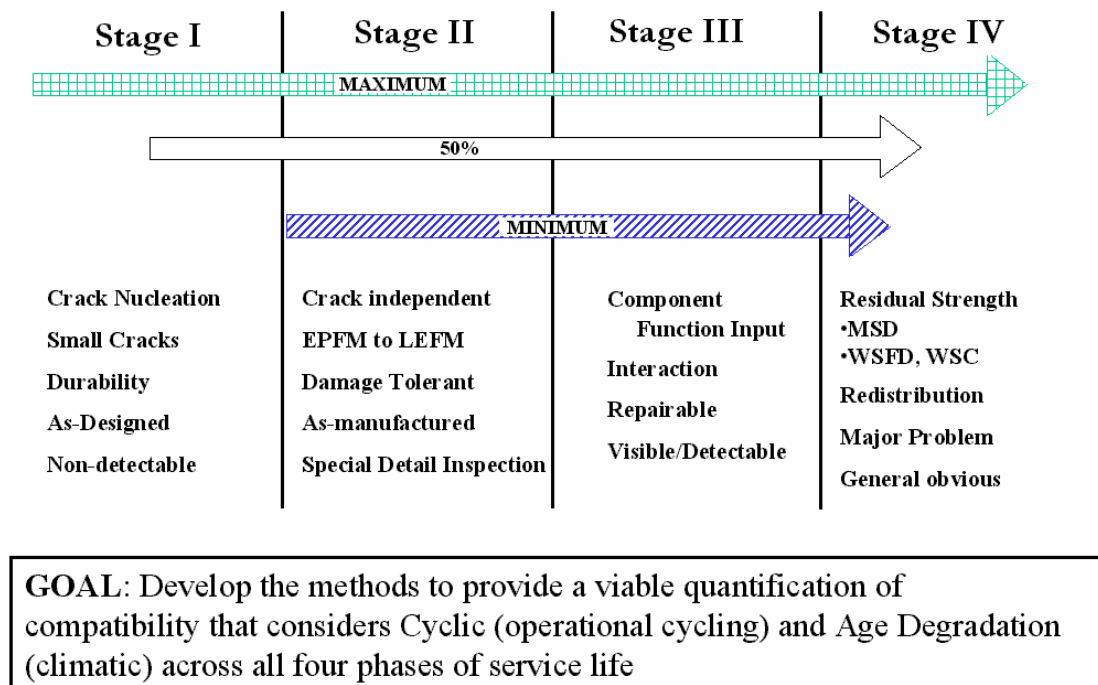


Figure 2 Holistic Approach Accounts for All Known Effects and Will Determine All States of Damage from Stage I (As-Manufactured) through Stage IV (Too Late).

2.0 PHASE I TASKS

This section describes our Phase I accomplishments. Phase I had the following objectives:

1. Identify state-of-the-art models for fretting fatigue life prediction that can be integrated with existing crack growth analysis methods;
2. Determine how to integrate fretting fatigue model(s) into crack growth analysis methods;
3. Establish an experimental program to develop the data necessary to implement and verify the fretting fatigue model(s).

2.1 Task I: Research Current Approaches

A literature review was the foundation of the analytical model development in Phase I of this SBIR project, with an emphasis on research conducted within the last 35 years. Experimental results and data, when available, along with the lessons learned, were evaluated for application. Fretting fatigue models developed in the past and currently in use (when published in the open literature) were scrutinized in order to avoid potential pitfalls and shortcomings of these models. Two high potential fretting fatigue modeling approaches were identified for incorporation into a holistic life prediction framework.

2.1.1 Early Experimental and Analytical Research

Fretting fatigue was first identified in 1910 and a great deal of progress has been made since that time in dealing with the complex phenomenon. Key references (3-8) discuss aspects of fretting fatigue that are relevant to these efforts.

Early efforts to assist the engineering community with robust analytical approaches were largely fruitless. However, during the 1950s two major approaches to dealing with fretting fatigue evolved (9-11): (1) a fretting fatigue life reduction factor and (2) testing components that represent actual joints to include the fretting fatigue phenomenon when dealing with the probable occurrence of fretting fatigue in use of components. Boeing uses a similar approach today in developing fatigue allowables and in the concept of the Detailed Fatigue Rating (DFR).

Numerous investigations in fretting fatigue continued during the 1960s. In 1968-69 Nishioka, et al. (12-17) introduced a quantitative approach to estimate the fretting fatigue allowable from stress and displacement approaches. Endo, Goto, and Nakamura in 1969 (18) studied the effect of environment on fretting followed by research into the interaction of fretting and corrosion. During the 1970's an understanding of the damage that resulted during the fretting fatigue process emerged. At the first International Symposium on Corrosion Fatigue held in 1971 both Waterhouse and Hoepfner (19-20) presented the concept of the fretting fatigue damage threshold. As well, Japanese researchers were beginning to apply fracture mechanics concepts to fretting fatigue life prediction.

The research of Endo and Goto (21) is important because they applied the concepts of fracture mechanics to fretting fatigue (See also 22). They may have been the first to formally do so but others were active at the time as noted. An early application of fracture mechanics to fretting fatigue was documented by Edwards at RAE (23), who observed that fretting crack nucleation life was approximately 25% of total coupon life and that the influence of

alternating stress did not completely explain the behavior of the fretted coupons. Edwards concluded that influences of frictional and normal contact tractions were dominant in fretting crack nucleation phase.

By 1981 Hoepfner had developed a holistic life prediction concept for pitting corrosion and fretting fatigue (25). The basic elements of the model are shown in Figure 3. Looking at the Figure 3 beginning at the left, one notes that if a pair of surfaces are in relative contact in some environment, under contact pressure and undergoing “small” relative displacement they will likely fret and create fretting damage. The first stages of damage are not necessarily cracking. After time, if the conditions to produce fretting fatigue exist, the damage will evolve. Eventually microscopic cracks form and may grow. Initially these cracks may be influenced by the contact force and friction, as concluded by Edwards (23). Also, the team headed by L. Vincent at University of Lyon in France has made extensive progress in assisting the understanding of the transition from initial fretting fatigue damage to propagating crack (26-35). However, none of the effort to date has yielded a functional relationship that allows a determination of the time/cycles for evolution of the initial damage state to a cracked state. This need for a functional relationship was one of the drivers in the development of the test matrix described in this report.

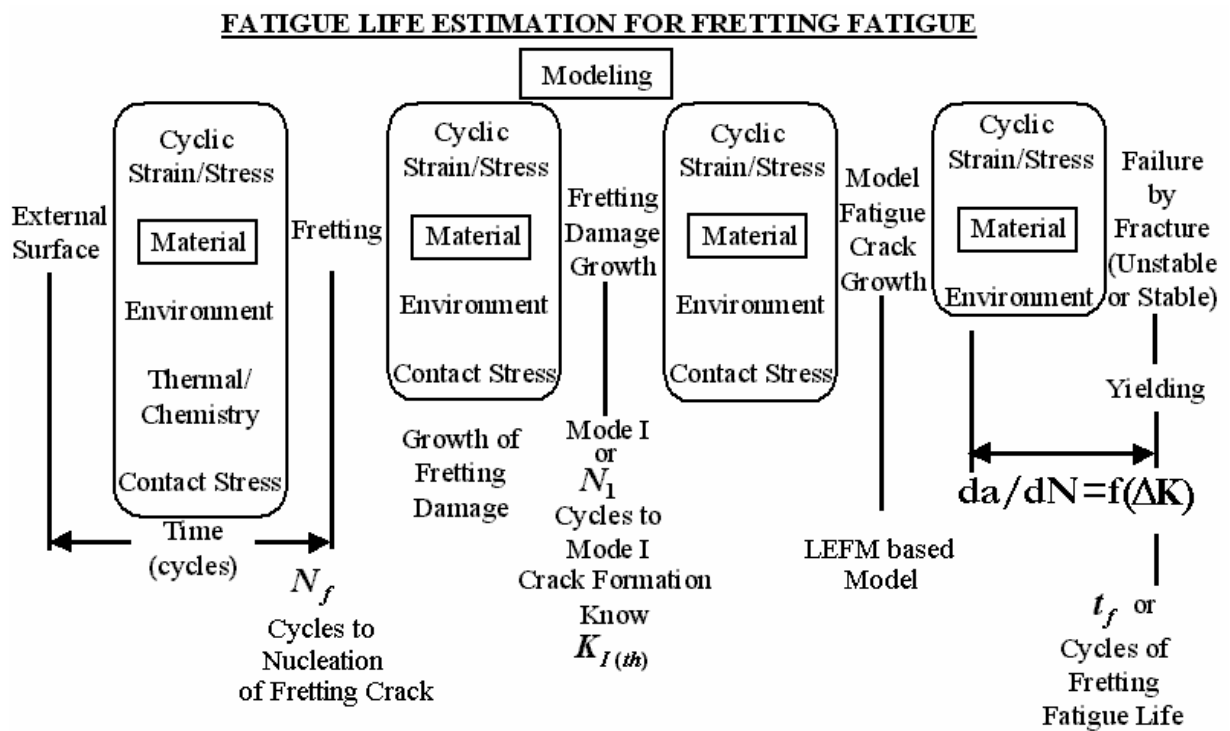


Figure 3 Fretting Fatigue Methodology.

2.1.2 Recently Developed Analytical Approaches

From 1980 to present, T. Hattori at Hitachi has applied the concepts of fracture mechanics to fretting life prediction extensively (36). Dr. Hattori and colleagues have studied fretting fatigue through use of both analytical and experimental methods (36-49), and have also developed design improvements meant to mitigate fretting influences (49).

In 1998, a group at the Massachusetts Institute of Technology (MIT) developed a ‘Crack Analogue’ approach to analyze fretting fatigue cracking under a flat rigid punch (50). The approach derives its methodology from the recognition that stresses at the corner of a flat punch are similar to stresses near the tips of edge cracks in infinite flat plates. Further, this model was extended in 2001 to the case of flat punch with rounded corners (51). This model will be described in more detail later in this report.

2.1.3 Non-destructive Testing (NDT)

Efforts to detect and quantify fretting with NDI techniques have been limited. The University of Dayton Center for Materials Diagnostics (52-55) has been studying fretting fatigue in aerospace engine alloys, specifically Ti-6Al-4V. Optical and acoustic microscopy based methods were used to characterize fretted surfaces. These methods require that the fretted surface be visible. Unfretted and fretted surfaces were examined with the white light interference microscopy (WLIM), which measured the surface roughness and asperity spacing and from these calculated the Power Spectral Densities (PSD) of the surface profiles. The PSDs were the metrics for comparing surfaces. A strong correlation existed in their measurements between the behavior of the PSD in full slip, partial slip, and stick regions, particularly when the PSDs of the fretted surfaces were normalized to the PSD of the original, unfretted surfaces. Though the WLIM method is a powerful technique for measuring PSDs of rough surfaces, it is not the only approach that will yield PSDs—PSDs can also be extracted from surface measurements made with x-ray and high resolution laser profilometry. While the results of this work were generally successful, it is not apparent how these methods could be applied to hidden surfaces.

Thermography has also been used on exposed fretted surfaces to attempt to measure fretting damage (56). Also, remote field eddy current has been used to measure material lost to fretting in a condenser tube-support plate structure, in a laboratory setting (57). No literature was found specifically concerning NDT for fretting on hidden surfaces, such as on the bore of fastener holes. There are NDT techniques that are promising for detection of fretting in fastener holes in controlled test situations. Acoustic emission (AE) techniques have been developed to distinguish between fretting and crack growth, and therefore AE may be useful in a controlled situation. Sonically-excited thermography may also be able to distinguish between fastener holes with and without fretting, by exciting further fretting and measuring the localized heating.

The transformation of the NDI fretting metrics to inputs of the life prediction methods presents unique challenges and significant hurdles that must be overcome in order to apply these methods to aircraft structure, whose fretted surfaces are most often not exposed but are hidden. Consideration and evaluation of NDI techniques need to be concurrent with predictive technology development.

2.1.4 Fretting Maps

Significant progress characterizing fretting damage has been made by the University of Lyon group headed by L. Vincent. Building on Vingsbo and Soderberg's work in a technique called 'fretting maps' (61), they have successfully been able to distinguish 'fretting damage modes' that are useful for identifying types of damage that may or may not occur in a fretting situation (27-35) by using measuring certain experimental parameters and constructing two 'maps', running condition fretting maps (RCFM) and material response fretting maps (MRFM), that are well correlated with surface and fretting cracking damage. These maps show that fretting damage can be separated into 3 'fretting modes', depicted on plots of shear stress against nominal displacement amplitude in Figure 4. The first mode, called 'stick mode' (Figure 4a), occurs in situations in which there is very little relative displacement (10 μm or less) between the fretting pad and the specimen, and is the least damaging. Generally very little damage to the integrity of the surfaces will be observed, and cracking due to fretting is never seen. The fretting pad and specimen are 'sticking' together and deforming elastically, so that very little plastic, permanent damage is done. The third fretting mode, 'gross slip mode' or 'sliding wear mode' (Figure 4c), is characterized by very large relative displacements (100 μm or more) between the fretting pad and the specimen. Any damage to fretted surfaces is usually confined to wear volume lost, and usually very little 'fretting induced cracking' is observed. The second fretting mode, the 'stick-slip mode' (Figure 4b), occurs when there is still small (approximately 20 μm to 70 μm) relative displacement between fretting pad and specimen, but is by far the most damaging of the three fretting modes. This method of plotting measured data is extremely useful as these maps allow one to discern fretting modes as the test is being conducted.

In addition to measurement of the shear stress and displacements, test coupon surfaces are examined under microscope and the surface damage characterized for non-degradation, cracking and particle detachment. The stress-displacement measurements and the surface damage characterization can be used to construct two 'fretting maps', both plotted on a normal contact load—nominal displacement graph. The first map, called the running condition fretting map (RCFM), uses the character of the shear-displacement hysteresis loops such as those in Figure 4 to distinguish the three fretting modes by correlating surface damage with slip-stick regions, Figure 5. Three distinct slip or stick regimes are distinguishable in Figure 5—a so-called 'sticking regime' or 'stick mode' (typically distinguished by no hysteresis loops), a 'mixed regime', or 'stick-slip mode' (typically distinguished by medium-sized hysteresis loops), and a 'gross slip regime' or 'gross slip mode' (typically distinguished by relatively large hysteresis loops). The mixed regime, it has been observed by Vincent (35) leads most often to fretting crack nucleation (or 'initiation'). The second map, called the material response fretting map (MRFM), Figure 6, uses measurements of surface degradation in the fretting pad and the specimen to separate non-degradation, cracking and particle detachment regimes, and is depicted on a graph that plots normal load against the relative slip of the fretting pad with respect to the fatigue specimen or coupon.

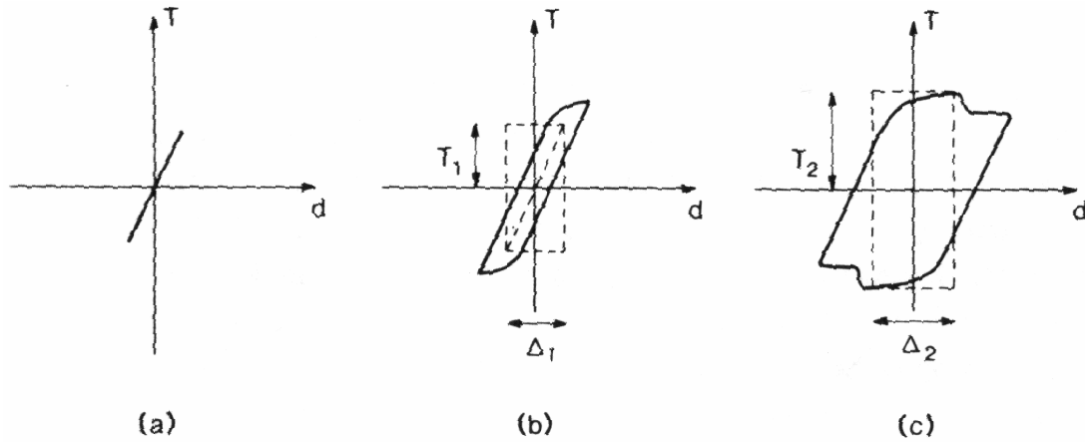


Figure 4 Shear and Displacements Measurements Allow Separation of Fretting Modes. Stick Mode Characterized by Elastic Deformations, Little Plastic Strain or Hysteresis. Stick-Slip Mode Characterized by Some Hysteresis. Full or Gross Slip Characterized by Large Hysteresis Loops. Vingsbo (61).

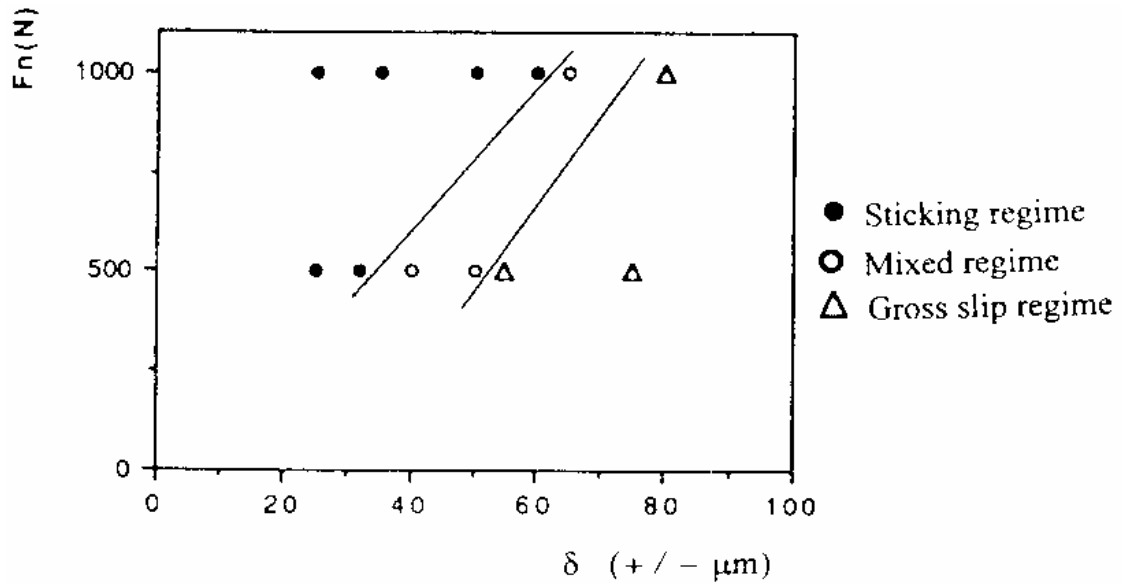


Figure 5 Running Condition Fretting Map (RCFM). Vincent (35).

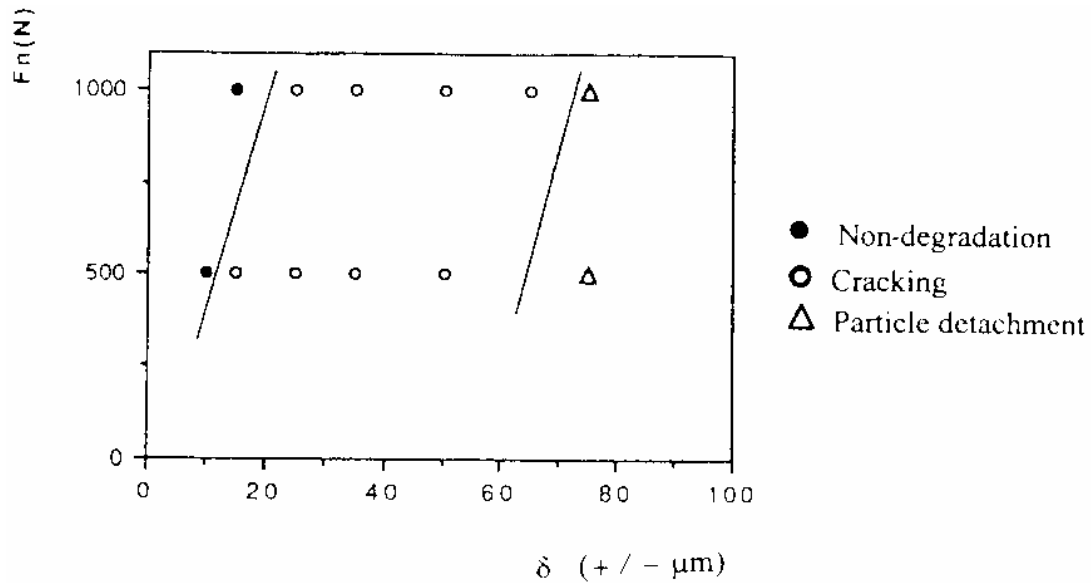


Figure 6 Material Response Fretting Map (MRFM). Vincent (35).

Correlated with the damage observed on fretted surfaces is the location of the fretting nucleated crack. Several researchers have noted a very strong correlation between the fretting crack nucleation site and the location of the stick-slip boundary (21, 62). Being able to predict the location of the stick-slip boundary therefore becomes an essential piece in the structural integrity prediction methodology. While fretting maps can be extremely useful for predicting stick-slip boundaries and hence fretting crack nucleation site, we have noted an extreme reluctance on the part of experimental test laboratories to adopt this technique, as successful execution of the fretting maps would require some financial investment in equipment and training. Alternative methods for distinguishing fretting modes are being used by test laboratories such as Alcoa. Alcoa is measuring scratch marks on fretted surfaces to attempt to discern damage modes, the idea being that the stick-slip boundary is often easy to distinguish once the coupon has been fretted a number of cycles.

2.2 Task II: Fretting Fatigue Candidate Model Development

Two fretting fatigue analytical approaches were identified during Phase I: the Hattori Model (36-49) and the Crack Analogue Model (50-51). Hattori's model is fracture mechanics-based model that adjusts the Mode I Stress Intensity Factor (SIF) ΔK_I for fretting conditions. Early versions of Hattori's model used the Rooke and Jones method for adjusting ΔK_I with the stress field (either analytical or finite element derived), while more recent versions use calculations of ΔK_I directly using the finite element or boundary element methods. The Crack Analogue Model is also fracture mechanics-based, but differs from Hattori's Model by using analytically derived SIFs ΔK_I that use the near equivalence of stress fields from well-known contact solutions to the stress fields near crack tips in certain configurations.

During the literature search (Task I), the large number of fretting fatigue models was pared down to two fretting fatigue models that were candidates for implementation; the one developed by Hattori's group at Hitachi of Japan (the 'Hattori Model', and the one developed at the Massachusetts Institute of Technology (the 'Crack Analogue' Model). These two models were selected because they: (1) were fundamentally sound, (2) were fracture mechanics based, (3) were easy to implement within our current damage tolerance framework, the Holistic Life Assessment Methodology, and (4) had some success correlating with experimental data.

2.2.1 Hattori Model

The 'Hattori Model' uses fracture mechanics based principles to calculate Mode I Stress Intensity Factors (SIFs) K_I . There are three parts to the Hattori Model (49): 1) stress singularity method, 2) estimation of threshold SIF K_{th} , and 3) fracture mechanics method. The stress singularity method is used to predict if and when a crack nucleates or 'initiates'. The threshold estimation procedure is used to adjust the threshold SIF K_{th} at stress ratio $R=0$ to other R -ratios. We will not be using either of these first two parts of the method. The stress singularity method is not needed because the Initial Discontinuity State (IDS) captures the physics of crack nucleation at constituent particles and their interface with the softer matrix material, (67)-(69). The threshold estimation procedure is not needed because tabulated crack growth rate data that varies with R -ratio will be used.

The fracture mechanics method has been applied to two-dimensional systems and will be used to predict the influence of the contact of the fretting pad against the substrate or coupon. The fracture mechanics method uses the Rooke and Jones (63) analytical solution for the influence of a point load (normal and shear) on the calculation of SIF for a crack of length 'a' located some distance 'x' away from the point load application, Figure 7, and extends this method to account for the variable pressure distributions that result from the contact of two bodies, Figure 8.

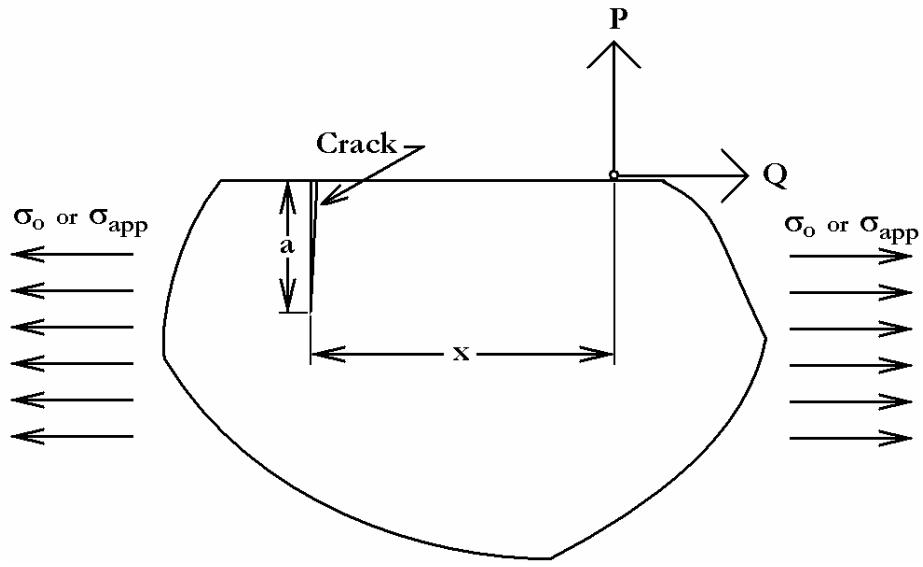


Figure 7 Fracture Mechanics Method Uses the Rooke and Jones Stress Intensity Factor Solution for Point Loads Effects.

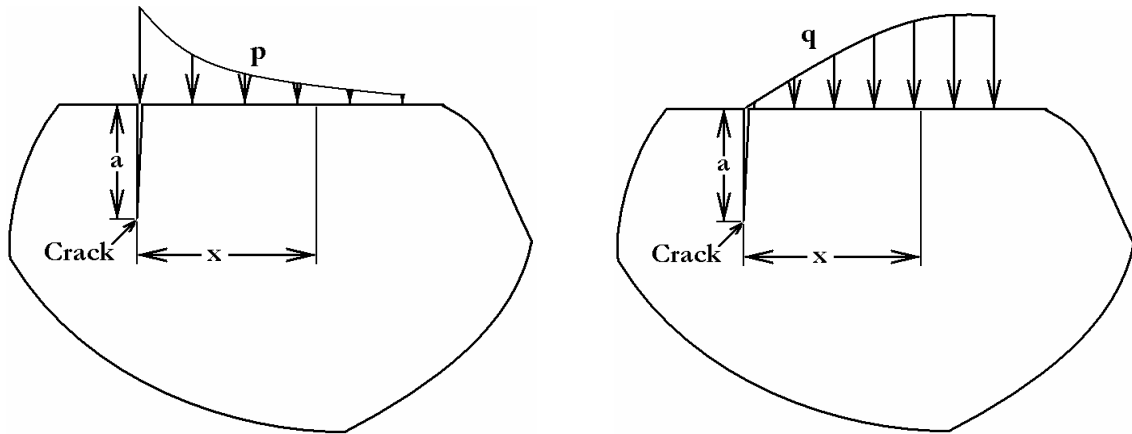


Figure 8 Fracture Mechanics Method Extends the Rooke and Jones Stress Intensity Factor Solution to Spatially Varying Amplitude Normal and Shear Traction.

The Rooke and Jones Stress Intensity Factor (SIF) solutions for point normal and shear loads located as indicated in Figure 7 have the following forms:

$$K_I(P) = \frac{P}{\sqrt{pa}} (1 - \mathbf{x}^2) \left[0.824 + 0.0637\mathbf{x} - 0.843\mathbf{x}^2 + 15.41\mathbf{x}^3 - 53.38\mathbf{x}^4 + 59.74\mathbf{x}^5 - 21.83\mathbf{x}^6 \right] \quad (1)$$

$$K_I(Q) = \frac{Q}{\sqrt{pa}} (1 - \mathbf{x}^2) \left[1.2943 + 0.0044\mathbf{x} + 0.128\mathbf{x}^2 + 10.89\mathbf{x}^3 - 22.14\mathbf{x}^4 + 10.96\mathbf{x}^5 \right] \quad (2)$$

with

$$\mathbf{x} = \frac{x}{x + a} \quad (3)$$

These are generalized to account for variable normal and shear tractions on the surface located some distance ‘x’ from a crack of length ‘a’, Figure 8.

$$K_I(p) = \int \frac{p}{\sqrt{pa}} (1 - \mathbf{x}^2) \left[0.824 + 0.0637\mathbf{x} - 0.843\mathbf{x}^2 + 15.41\mathbf{x}^3 - 53.38\mathbf{x}^4 + 59.74\mathbf{x}^5 - 21.83\mathbf{x}^6 \right] dx \quad (4)$$

$$K_I(q) = \int \frac{q}{\sqrt{pa}} (1 - \mathbf{x}^2) \left[1.2943 + 0.0044\mathbf{x} + 0.128\mathbf{x}^2 + 10.89\mathbf{x}^3 - 22.14\mathbf{x}^4 + 10.96\mathbf{x}^5 \right] dx \quad (5)$$

The Stress Intensity Factor due to the far field applied stress \mathbf{s}_0 is calculated from

$$K_I(\mathbf{s}_0) = 1.122\mathbf{s}_0\sqrt{pa} \quad (6)$$

The total Stress Intensity Factor due to the fretting and the far field applied stress is calculated from a superposition of Equations (4), (5), and (6) to model the mechanical system shown in Figure 9.

$$K_I(\mathbf{s}_0, p, q) = K_I(p) + K_I(q) + K_I(\mathbf{s}_0) \quad (7)$$

Note that all equations have been derived by Hattori for through cracks. Modifications to the normal and shear contact pressure Stress Intensity Factor Equations (4) and (5) to account for part-through crack scenarios need to be made.

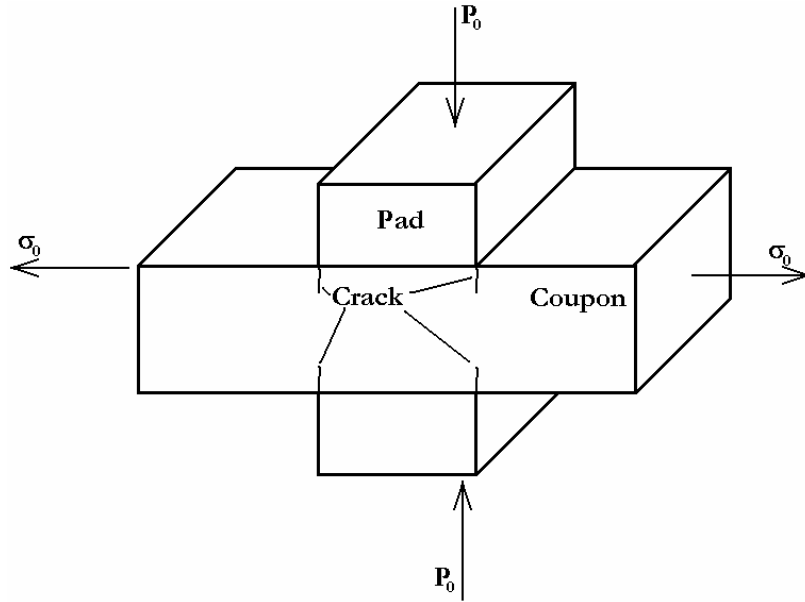


Figure 9 Fracture Mechanics Method Models the Fretting Pad with Normal and Shear Contact on Fatigued Coupon.

Wear of the fretting pad causes the contact point between the pad and substrate to shift away from the crack. This shift in contact point is accounted for by introducing a crack wear model of the type postulated by Archard (64):

$$V = K \frac{pS}{3H} \quad (8)$$

where: V is the wear volume, in³
 K is the wear coefficient, in⁴*lb⁻¹
 p is the contact pressure, psi
 S is the relative displacement, in.
 H is the hardness.

Hattori's model accounts for the inclined orientation of the typical crack nucleated by fretting fatigue by first computing the uncracked stress state using finite element software, locating the loci of maximum stress at different depths into the substrate, and using the loci to define the crack angles in subsequent finite element analyses that compute the Mode I SIFs needed for the crack propagation analyses.

Though the Hattori model has been tested only with two-dimensional fretting pad and coupon configurations, the method is a very flexible, fracture mechanics based approach that should work for fretting with an arbitrary geometry.

2.2.2 Crack Analogue Model

The ‘Crack Analogue’ model was introduced by Giannakopoulos, et al. in 1998 (50) for the case of a rigid flat punch indenting or contacting a large or semi-infinite substrate. The approach derives its methodology by recognition that the closed form analytical stress fields near the corner where a flat punch contacts the substrate, where fretting cracks are known to nucleate, asymptotically approach the closed form analytical stress fields near the tips of edge cracks located in infinite flat plates subject to normal and shear point loads located far field from the crack tips.

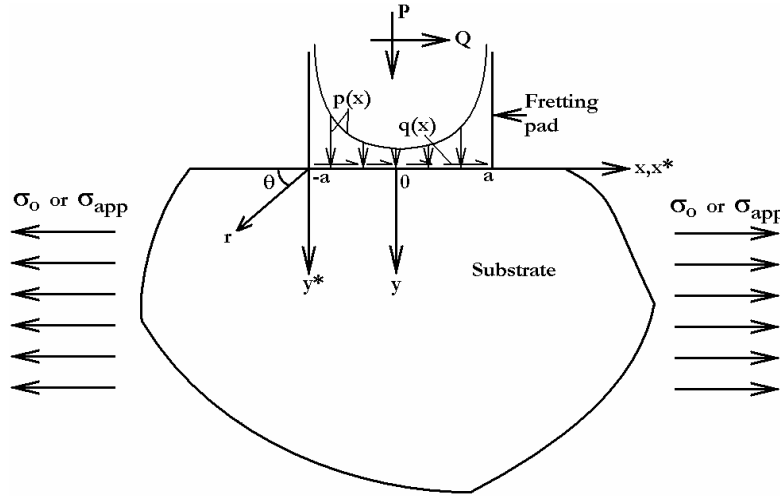


Figure 10 ‘Crack Analogue’ Model Uses the Asymptotic Stress Field as the Pad (or Punch) Corner is Approached ($r \rightarrow 0$) in the Substrate.

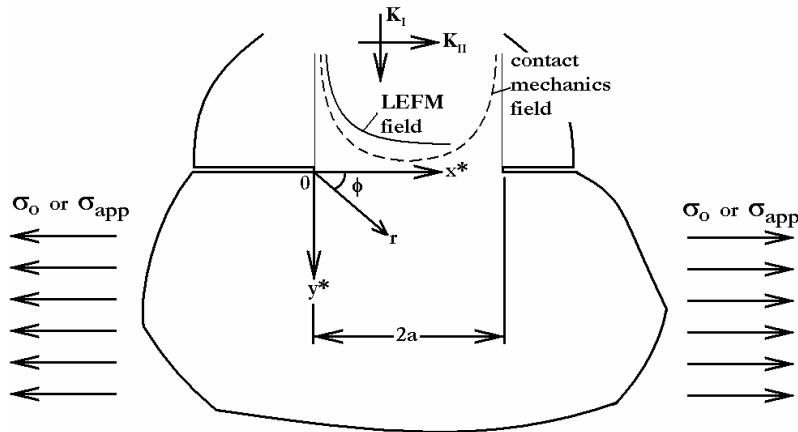


Figure 11 ‘Crack Analogue’ Model Uses the Asymptotic Stress Field at the Crack Tip in a Double-Edge Crack in Semi-infinite Body Loaded by Point Normal and Shear Loads at Infinity.

The asymptotic stress fields in the substrate near the corner of the flat punch can be shown to have the following form (see Figure 10 for nomenclature):

$$s_{yy} \approx -\frac{P}{p\sqrt{2ar}} \text{ as } r \rightarrow 0 \quad (9)$$

$$s_{xy} \approx \frac{Q}{p\sqrt{2ar}} \text{ as } r \rightarrow 0 \quad (10)$$

where: P is the normal load on the pad, lbs/in.

Q is the shear load on the pad, lbs/in.

a is the poker half-width, in.

r is the radial distance in the substrate from the corner of pad, in.

The asymptotic stress fields near the two edge crack tips in an infinite body loaded with a normal load P and a shear load Q at infinity can be shown to have the following form (see Figure 11 for nomenclature):

$$s_{yy} \approx \frac{K_I}{\sqrt{2pr}} \text{ as } r \rightarrow 0 \quad (11)$$

$$s_{xy} \approx \frac{K_{II}}{\sqrt{2pr}} \text{ as } r \rightarrow 0 \quad (12)$$

where: K_I is the Model I Stress Intensity Factor, psi-in^{1/2}

K_{II} is the Model II Stress Intensity Factor, psi-in^{1/2}

r is the radial distance in the substrate from the crack tip, in.

In the limit as the edge of the punch is approached and the crack tips are approached, the stress fields are equivalent.

$$K_I = -\frac{P}{\sqrt{pa}} \text{ as } r \rightarrow 0 \quad (13)$$

$$K_{II} = \frac{Q}{\sqrt{pa}} \text{ as } r \rightarrow 0 \quad (14)$$

These two equations are used to describe the growth of an inclined crack from one of the edge crack tips in the infinite body in Figure 12 below. Arbitrarily, the origin of the inclined crack is located at the left crack tip in Figure 12.

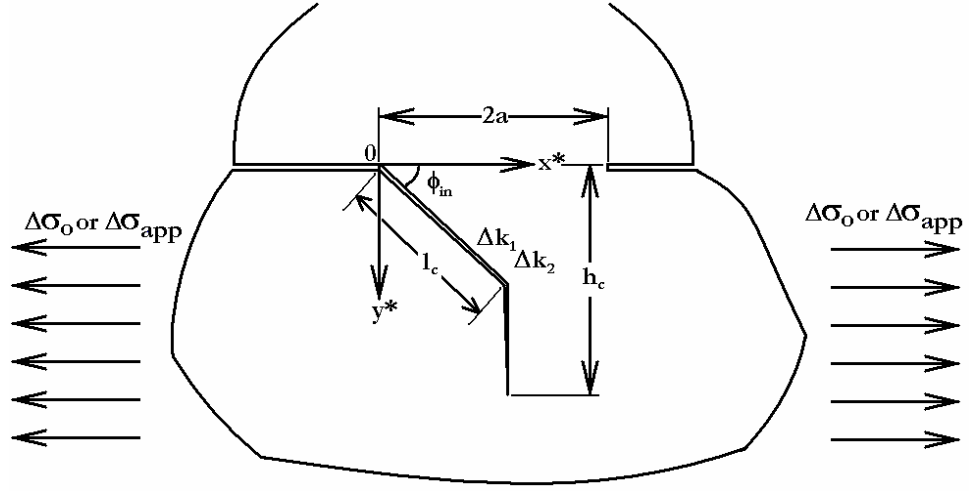


Figure 12 ‘Crack Analogue’ Cracking Scenario Consists of Constant Inclination Crack Originating at Crack Tip that ‘Kinks’ or Turns When the Stress Intensity Factor Due to the Far Field Stress is Larger than the ‘Local’ Stress Intensity Factor at Inclined Crack Tip.

The inclined crack grows entirely under the influence of the fretting at a constant angle f_{in} that can be derived by setting the ‘local Mode II stress intensity factor’ k_2 as described by Suresh (70), to θ . The local Mode II stress intensity factor is a function of the crack slant angle, and the ‘global’ Mode I and Mode II SIFs, K_I and K_{II} , respectively, which themselves are functions of the applied normal and shear loads, respectively:

$$k_2 = \frac{K_I}{4} \left(\sin\left(\frac{f_{in}}{2}\right) + \sin\left(\frac{3f_{in}}{2}\right) \right) + \frac{K_{II}}{4} \left(\cos\left(\frac{f_{in}}{2}\right) + \cos\left(\frac{3f_{in}}{2}\right) \right) \quad (15)$$

The angle f_{in} is found rearranging Equations (13)-(15), then using a numerical iteration technique such as Newton-Raphson and solved *a priori* for f_{in} as a function of the friction coefficient m :

$$\left(\sin\left(\frac{f_{in}}{2}\right) + \sin\left(\frac{3f_{in}}{2}\right) \right) \left[\cos\left(\frac{f_{in}}{2}\right) + 3\cos\left(\frac{3f_{in}}{2}\right) \right]^{-1} = \frac{Q_{max}}{P} = m \quad (16)$$

The crack grows under the influence of a ‘local stress intensity factor’ Δk_1 with the following form:

$$\Delta k_1 = \pm \frac{3}{4} K_{II} \Big|_{max} \left(\sin\left(\frac{f_{in}}{2}\right) + \sin\left(\frac{3f_{in}}{2}\right) \right) \quad (17)$$

The length l_c is found by using the following relation for a doubly-kinked crack (65):

$$K_{th} = \frac{\Delta S_{app} \sqrt{p l_c}}{4} F(f_{in}) \quad (18)$$

where

$$F(f) = F_1(f) \left(3 \cos \left(\frac{p - 2f_{in}}{4} \right) + \cos \left(\frac{3(p - 2f_{in})}{4} \right) \right) + 3F_2(f) \left(\sin \left(\frac{p - 2f_{in}}{4} \right) + \cos \left(\frac{3(p - 2f_{in})}{4} \right) \right) \quad (19)$$

$$F_1(f) \approx 1.058 \sin(f) - 0.065 \sin(3f) \quad (20)$$

$$F_2(f) \approx 0.374 \sin(2f) + 0.023 \sin(4f) \quad (21)$$

When the inclined crack reaches l_c in length, the Mode I crack opening mechanism due to the bulk stress ΔS_{app} then overtakes that of the fretting, and the crack becomes a vertical crack growing into the substrate, Figure 12. Crack propagation continues until the specified failure criterion is met: the net section yields, K_{IC} is reached, or some other criterion specified by the analyst.

This method has been extended to the analogy between the asymptotic stress fields near the corners of a rounded flat punch and the asymptotic stress fields near the tip of a blunt crack (51).

2.3 Task III: Development of Fretting Fatigue Test Plan

This Phase I Task defined the goals, success criteria, protocol, procedures, testing standards, and the parameter space (or matrix) of an experimental fretting test program that will supply the data needed for analytical model development. The resulting data foundation provides the building block toward subsequent validation and demonstration.

There are four distinct activities that are useful for validating analytical life prediction methods for our fretting fatigue models: 1) correlation of analytical methods with experimental test data, 2) comparison of Stress Intensity Factors (SIFs) computed with finite element software against the Rooke and Jones methods summarized in Equations (4) and (5) in **Section 2.2.1** above, 3) correlation of finite element method simulations and normal contact pressures measured with the Fuji film technique, and 4) finite element method simulations of the complex, three-dimensional states of stress in the Single Rivet Lap Joint (SRLJ), with special emphasis on friction effects.

The activities of this task resulted in the description of an experimental test program that will successfully accomplish the first validation activity described above. The experimental part of the third validation activity is also described in this section. The second and fourth validation activities are described in **Section 2.4 Task IV Fretting Fatigue Model**

Integration below. The computational part of the third validation activity is also described in **Section 2.4**.

Two types of tests are described in this section: 1) Non-destructive testing (NDT) and 2) Fretting Fatigue Tests. The NDT experiments serve two purposes: 1) determination of fretting damage detection levels and 2) validation of normal contact pressures calculated with finite element methods. NDT is an integral part of any aircraft maintenance program; therefore, consideration and evaluation of NDT techniques should be concurrent with predictive technology development to make sure any tool delivered to military and commercial customers fits within customers' existing Structural Integrity Programs.

2.3.1 Non-destructive Detection of Fretting

Non-destructive detection of structural damage is a vital part of life cycle maintenance programs for aircraft—information about the damage state in the existing structure is needed to evaluate the existing safety in the aircraft and is also needed as input into life prediction methods that are used to estimate the remaining service life of the structure. Currently, the arsenal of common Non-destructive Testing (NDT) techniques includes eddy current, pulsed eddy current, X-ray, and ultrasound. Each technique works better for specific types of damage in certain structural elements. However, none of these techniques works well for detecting fretting and fretting fatigue. Admittedly, detection of fretting and associated damage is a very difficult task, as fretting occurs on hidden surfaces that are most often located at fastened joints (detection of damage at the fastener hole is particularly challenging). Recently, other NDT techniques such as thermography have become available that show some promise for reliable detection of the fretting damage.

2.3.1.1 Conventional Non-destructive Testing

As stated in the **Section 2.1.3 of Task I** above, there are very few methods for detecting fretting that have been documented in the open literature. There are two Non-destructive Testing (NDT) techniques that are promising for detection of fretting in fastener holes in controlled test situations. Acoustic emission (AE) techniques have been developed to distinguish between fretting and crack growth, and therefore AE may be useful in a controlled situation. Sonically-excited thermography may also be able to distinguish between fastener holes with and without fretting, by exciting further fretting and measure a resulting localized heating. The methods appear to be most useful, though have limited capability for distinguishing fretting damage on hidden surfaces.

To determine the capability of different Non-destructive Inspection (NDI) techniques for detecting fretting, a number of simple lap joints (containing one rivet) will be used. The simple lap joints should be subjected to cyclic loading and the joint monitored with different NDI techniques (particularly Thermography). Once NDI detects something, the joints can be disassembled see what damage is present. The number of cycles would then be increased or decreased to see the type of damage present. A large number of specimens would be required to do this work but since they are simple lap joints, the cost to manufacture the specimens will be relatively small. With the assistance of fractography, these specimens can also be used to help determine how fretting pits form, and do constituent particles get pulled and cause fretting or does an oxide layer build up and then break down?

2.3.1.2 Fuji Film Tests

Validation of normal contact pressures calculated with finite element methods, described in somewhat more detail in **Section 2.4.3** below, will be accomplished with an experimental study that experimentally measures normal contact tractions between two skins clamped together with a technique called the Fuji Film Contact Pressure Method.

A small experimental study previously carried out by NRCC will be described. Fuji pressure sensitive film was sandwiched between two thin sheets of aluminum, and rivets were installed to assemble the single riveted lap joint (SRJL) specimens.

Fuji pressure sensitive film is a two part medium consisting of an A-film and a C-film both having an active coating placed overtop a polymer substrate. The active surface of the A-film consists of microscopic bubbles of varying sizes within which are contained a proprietary liquid. When pressure is applied to the film a number of bubbles burst releasing a liquid that reacts with chemicals in the C-film to produce a pink stain. The optical density of the stain can be directly correlated to the applied pressure. In this way Fuji pressure sensitive film enables for both the contact area and contact pressure to be determined. Figure 13 below shows a schematic of the film:

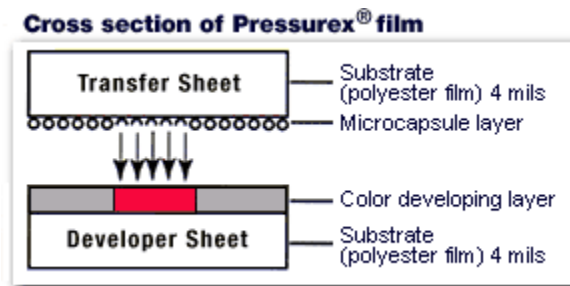


Figure 13 Fuji Pressure Sensitive Film Is Two-Part Medium.

Table 1 below shows the discrete pressure ranges that are available for the pressure sensitive film. Fuji film in the low, medium and high pressure ranges was used for the initial experiments. This allowed for pressure measurements as low as 350 psi (low film) and as high as 18,500 psi (high film). Three single rivet lap joint (SRLJ) samples were prepared with only one central rivet. Sheets of pressure sensitive film in the various pressure ranges were cut to size and inserted between the front and back faces. The samples were then riveted and the film was allowed to develop for five (5) minutes before disassembly. Drilling out the rivet with a slightly undersized drill bit allowed for removal of the pressure sensitive film. The experiment was then repeated sandwiching all three film types together and placing them between the front and back face of a SRLJ. Figure 14 and Figure 15 show a SRLJ specimen with the pressure sensitive film sandwiched between the front and back face.

FILM SPECIFICATIONS	
FILM TYPE	PRESSURE RANGE
Pressurex Micro	2 - 20 PSI (.14 - 1.4 kg/cm ²)
Ultra Low	28 - 85 PSI (2 - 6 kg/cm ²)
Super Low	70 - 350 PSI (5 - 25 kg/cm ²)
Low	350 - 1,400 PSI (25 - 100 kg/cm ²)
Medium	1,400 - 7,100 PSI (100 - 500 kg/cm ²)
High	7,100 - 18,500 PSI (500 - 1300 kg/cm ²)

Table 1 Pressure Ranges for Pressure Sensitive Film.



Figure 14 SRLJ Specimen Top View.

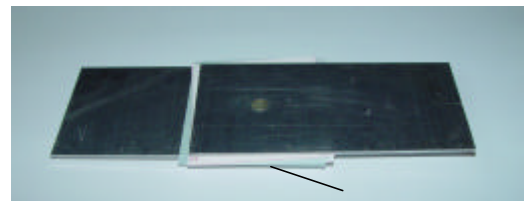
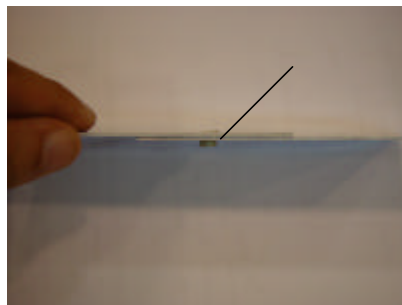


Figure 15 SRLJ Side View. Note Pressure Sensitive Film Sandwiched Between Both Layers (arrows).

For the initial pilot study the goal was simply to verify whether a pressure distribution could be obtained from a SRLJ specimen and whether the pressure sensitive film would be damaged upon rivet removal. Figure 16 shows the results of the initial testing.

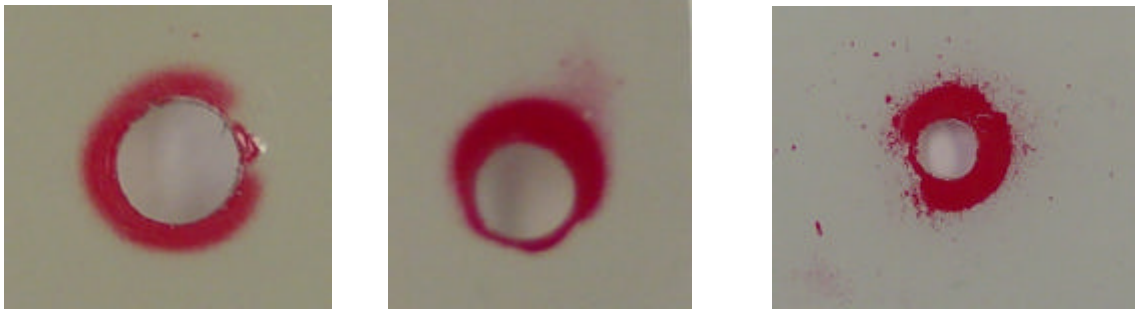


Figure 16 Individual Results - High, Medium and Low Film (Left to Right).

Figure 17 shows the results from the test with all three film grades sandwiched in the SRLJ at the same time:

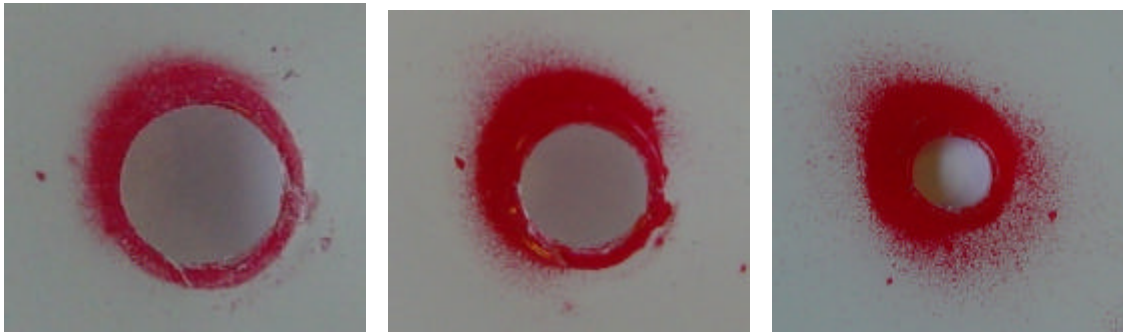


Figure 17 Sandwich results – High, Medium, and Low Film (Left to Right).

Although the results of this particular analysis are not calibrated, some interesting information can certainly be ascertained. Although the low pressure film (Figure 17 right) appears to be over-exposed, it does give us the best idea of what the actual contact area is. Low pressure film does not respond below 350 psi, therefore an even lower grade could be used to determine contact pressures/areas below this threshold. The medium pressure film (Figure 17 center) provides the least information, since it is oversaturated and only provides contact area/pressure information in the range from 1400-7100 psi. Of interest is the fact that the basic shape of the contact patch remains generally unchanged in all three images. The high pressure film (Figure 17 left) can provide the best estimate of contact pressure. Since the film is not overexposed the pressure must be somewhere in the range from 7100 – 18,500 psi. Given the intensity of the red, a rough approximation would put the pressure half way between the upper and lower limit, approximately 13,000 psi. Once the film has been calibrated, pressures at intervals of 0.5 MPa or less can be calculated with much greater certainty. Accurate measurements of the contact area could be made as well. The results from

the single film tests show similar results. The stain pattern is more circumferentially uniform suggesting that the rivet placement was more accurate. Both the low and medium films are over-exposed, while the high film shows an intermediate red intensity. This NRCC study demonstrated the feasibility of using pressure sensitive film to measure the load distribution between the front and back sheet.

Additional work is necessary in order to provide more quantitative results for the pressure distributions. Initially, ten (10) joints with only one rivet installed (the SRLJ) will be used to test the ability of the Fuji film to measure contact pressure. Controlled force riveting will be used to assemble the SRLJs after insertion of the Fuji pressure film. Riveting force levels will be varied to establish the relationship between the riveting force and the contact pressure. To improve interpretation of the Fuji film indications, a careful calibration of the film and its colors will be conducted. The calibration procedure for pressure sensitive film involves placing the film in a punch and creating stains at various load levels. By measuring the diameter of the punch and by recording the maximum load level, it is possible to calculate the applied pressure. When the individual stains are then digitized it is possible to correlate image intensity to applied pressure. After each stain is developed a CCD camera can be used to capture the image. Each image can be translated into grayscale and the contact area as well as the pressure distribution can be determined using image processing software. Experimentally measured residual stress fields obtained in a previously completed NRCC study must be used to relate the rivet load to the contact pressure in the SRLJ.

If time and funding permits, additional tests could be conducted using a Multiple Rivet Lap Joint (MRLJ) with three rows of five rivets as seen below in Figure 18. Again, experimentally measured residual stress fields such as those from a previously completed study must be used to relate the rivet load to the contact pressure to the residual stress present in this complex MRLJ.

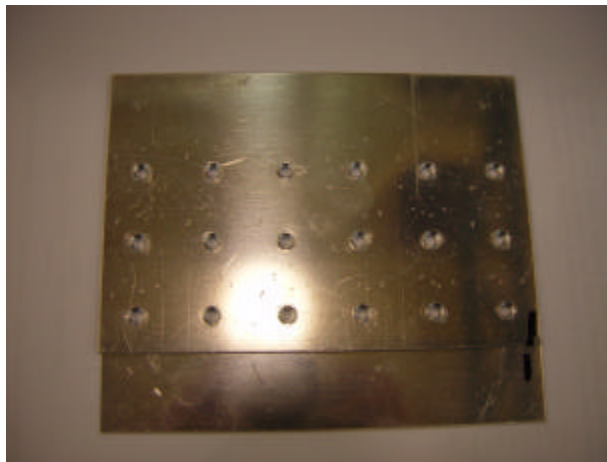


Figure 18 Fifteen-Rivet Lap Joint to Be Tested.

2.3.1.3 NDT Tests in Lap Joints

The sensitivity of the various NDT techniques toward levels of fretting on hidden surfaces will be tested. About 10 test specimens will be cycled while being monitored with thermography. In sequence, specimens to be removed from test upon unusual thermographic indication, or upon reaching a milestone number of cycles, whichever comes first. Each subsequent specimen shall be carried over beyond the removal criteria of the previous specimen. Each specimen shall then be inspected using vibro-thermography, pulsed eddy current and immersion UT leaky wave and other techniques prior to disassembly. In addition, the specimen will be inspected by X-ray to determine its ability to detect fretting debris prior to teardown. Optical analysis of fretting, or other damage to be correlated to the NDI results.

2.3.2 Fretting Fatigue Test Program

An extensive experimental test program that will be used to validate and verify the analytical life prediction approaches is described.

Research in fretting fatigue has revealed many important parameters that influence fatigue performance, in no particular order:

Materials	Temperature
Bulk stress	Notch effects
Normal contact stress	Slip amplitude
Contact shear stress	Chemical environment
Friction coefficient	Surface treatment
Poker displacement in bulk stress direction	Frequency
Poker geometry (length, corner radius, etc.)	

A complete test matrix that evaluates all of these parameters is monumental, from both an engineering and financial perspective. Therefore, for the first priorities, we have focused on parameters that are most prevalent in external aircraft structure, particularly riveted aircraft lap joints. Riveted joints are prime fretting fatigue candidates because of extensive areas of contact between fasteners and the bores of fastener holes, and between faying surfaces of the joint. A building block approach was used to define the test matrix in this Task, Figure 19. The building block approach introduces important parameters in a controlled fashion before moving on to the complexities of a true joint. Coupon tests, at the bottom of the pyramid, are conducted to determine basic material properties, normally using standard coupon designs. Element tests, using non-standard coupons, introduce new variables that more closely represent the target aircraft structure. Typical Configuration tests involve more complex structural details than element tests (such as a ‘representative lap joint’). Sub-components are tests of substructures that are actual aircraft structure. Full-Scale tests examine fatigue in full-scale, production structure.

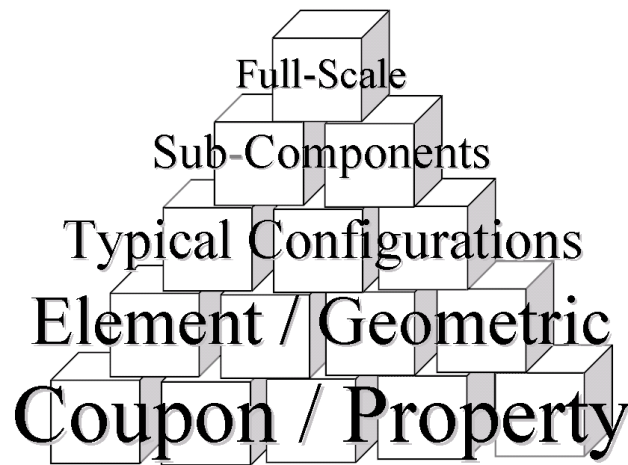


Figure 19 Building Block Approach Requires Validation of Analytical Methods with Simple Coupon Tests first, Then Element/Geometric Tests, etc.

The overall objective of the test program is to secure fretting fatigue data that can be used to correlate with the analytical life prediction models for fretting fatigue configurations that are representative of aircraft structure. For instance, fretting degradation is strongly dependent on the material types of the fretted structures. The fretted structures in aircraft typically are aluminum, either 2000 or 7000 series; therefore tests with 2000 or 7000 series aluminum alloys that are representative of typical aircraft construction materials are defined. One major goal of the test program is to be able predict, via understanding the stress state, the likelihood of the presence of a stick-slip interface and its location.

A multi-tiered, building block approach is proposed. Key elements of the test program, in increasing levels of complexity, are:

- Baseline, low K_t fatigue experiments (no fretting)
- Fretting fatigue, low K_t experiments
- Fretting fatigue, high K_t experiments
- Pressure contact measurement riveted joint, Fuji pressure-sensitive film
- Fretting fatigue, simple element test (single rivet lap joint-SRLJ)
- Fretting fatigue, complex element test (multi-rivet lap joint-MRLJ)

The test matrix is summarized in Table 2 below, in which the test types and the test goals are briefly stated. Each test will be briefly described below.

Test	Test Goal
IDS	Baseline Characterization of Material
Low Kt	Fretting Fatigue Behavior in Low Kt Coupons
High Kt	Fretting Fatigue Behavior in High Kt Coupons
Single Rivet Lap Joints	Simple element test
Multiple Rivet Lap Joints	Complex element test

Table 2 Proposed Test Matrix

2.3.2.1 IDS Characterization of Material (Baseline fatigue)

It is important to establish baseline fatigue behavior in the test materials at the test stresses. Coupon design is a simple dog bone with nominal $K_t = 1$ (the term ‘low K_t ’ will be used hereafter to describe similar coupons) and test procedures will follow ASTM Standard E466 for Constant Amplitude Fatigue Testing for Aluminum Alloys. The test material will be 0.063 inch bare 2024-T3 aluminum, a common lap joint material for aging transport aircraft in both commercial and military service.

A total of 18 coupons are required for this sub-series, six at each of two stress levels and three each at two stress levels, Table 3. Run-out, or test termination barring fracture, will be capped at 5,000,000 cycles, and this may be approached for the 30 ksi coupons in particular. When fretting is introduced in the next sub-series, lives will decrease substantially. The tests will be monitored for cycles to failure (N_f), and if fracture occurs, the initial discontinuity state (IDS—most often a second phase particle in this type of material) will be measured. The location of the crack origin will also be carefully documented.

The only variable in these tests is the max alternating fatigue stress applied, 30 and 40 ksi. All tests will be conducted at 10 Hz in laboratory air of no more than 40% RH and 75 °F.

Material	Stress Level (max ksi)	Stress Ratio	Replicates	Measured Parameters
2024-T3	30	0.02	6	N_f , IDS
2024-T3	35	0.02	3	N_f , IDS
2024-T3	40	0.02	6	N_f , IDS
2024-T3	45	0.02	3	N_f , IDS
		Total Coupons	18	

Table 3 Test Matrix for Baseline Fatigue Behavior.

2.3.2.2 Fretting Fatigue Behavior in Low Kt Coupons

In this sub-series of tests, a number of variables will be investigated to determine their influence on the fretting fatigue behavior of AA 2024-T3. Two sets of tests will be performed: 1) ‘bench’ or pilot tests to improve future fretting tests and 2) ‘main’ tests that will fulfill prediction model data needs.

Coupon geometry and certain test conditions (testing frequency, R, environment) will be identical to the baseline coupons with added requirement that a flat or cylindrical fretting pad be in contact with the center of the gauge section to set up fretting conditions. Normal load will be controlled with using a bolt threaded into a load cell. In this way, normal load can be consistently adjusted for each test, and any fluctuation of the normal load can also be monitored.

a) Bench Test Matrix

The effects of wear and tangential load will be investigated in a reduced ‘bench’ or pilot test matrix, Table 4. Wear effects will be investigated by a small investigation of the research in the field in this area, querying experts for their field experience, and conducting a small pilot study with replicates shown in Table 4 below. In the wear study, fretting pads will be changed frequently at specified intervals and fretting pads sectioned to measure the worn fretting pad contours.

Tangential load effects will be studied with a small pilot study that will use two different surface roughness, an ‘average’ or nominal surface roughness and a ‘highly polished’ surface roughness, on the fretting pads. (Note a consistency between conditions with Table 5 tests.)

Material	Stress Level (max ksi)	Stress Ratio	Punch Geometry	Normal Pressure (psi)	Wear Study	Tangential Load Study
2024-T3	30	0.02	Cyl	8000	2	2
2024-T3	30	0.02	Flat	8000	2	2
2024-T3	40	0.02	Cyl	13000	2	2
2024-T3	40	0.02	Flat	13000	2	2
		Total Coupons			8	8

Table 4 Bench Test matrix for Low Kt fretting fatigue.

b) Main Test Matrix

After completion of the Bench Test Matrix, the main test matrix will be completed. The Main Test Matrix is designed to capture prediction model data needs for low Kt structures. Characterization of fretting fatigue damage is a complex issue and requires that a number of parameters be measured. For instance, it will be necessary to interrupt the tests and characterize the surface damage before progressing in some cases. The proposed fretting matrix is shown below in Table 5.

Test variables include:

- Normal Pressure
- Alternating Fatigue Stress
- Contact Pad (Punch) Geometry
- Cycles to Interrupt

The alternating fatigue stresses are the same as the baseline stresses.

Normal pressures have been picked to simulate contact pressures in a lap joint as estimated from the Fuji film contact pressure study references elsewhere in this report. A normal pressure of 13,000 psi is sought for one level. A lesser level of 8,000 psi will also be used as a comparison point. Contact pressure cannot be made too high, or contact will be in a stick condition only, which will not produce fretting fatigue.

The contact pads will be made in two geometries, flat contact and cylindrical contact. This provides two geometries and contact stress types for use in model development and data correlation in later tasks. Note: The first conditions tested will be cycles to failure (i.e., no interruption) at the different stresses. If no appreciable difference is detected between pad geometries, then one can be eliminated for the interrupted test matrices, thereby considerably shrinking the overall test matrix. All the tests to failure will be monitored for visible cracking, or other non-destruction examination, and then the damage measurements made. Post-failure analyses and examinations will be performed on all specimens.

Some of the tests will be interrupted prior to failure and the damage will be thoroughly characterized. The surface will be scrutinized for cracks and morphology of the fretting scars will be determined and location of the stick/slip interface. Correlations will be sought between the location of this interface and the location of the primary crack. Crack nucleating discontinuities will be examined using fractographic techniques on post-fracture surfaces.

If cracks are detected, two of the coupons will be broken open, and two will be metallographically sectioned to reveal crack profile, and two will be subjected to a fracture surface marking sequence and then tested to failure or run-out with normal load removed.

For the coupons that are polished to reveal the crack profile, this will make it possible to get very accurate crack angles as a function of depth (this is important for use in stress intensity calculations and for model verification).

Responses to be measured include:

- Cycles to failure (where applicable)
- Location of stick/slip interface
- Location of cracking relative to that interface
- Slip amplitude (determined by measuring fretting scars on the surface)
- Fractographic features (transition depths of slant to normal fracture, crack origins)

Material	Stress Level (max ksi)	Stress Ratio	Punch Geometry	Normal Pressure (psi)	Replicates	Interrupt Level
2024-T3	30	0.02	Cyl	8000	6	Nf
2024-T3	30	0.02	Cyl	8000	6	50%
2024-T3	30	0.02	Cyl	8000	6	25%
2024-T3	30	0.02	Cyl	8000	6	10%
2024-T3	30	0.02	Flat	8000	6	Nf
2024-T3	30	0.02	Flat	8000	6	50%
2024-T3	30	0.02	Flat	8000	6	25%
2024-T3	30	0.02	Flat	8000	6	10%
2024-T3	40	0.02	Cyl	13000	6	Nf
2024-T3	40	0.02	Cyl	13000	6	50%
2024-T3	40	0.02	Cyl	13000	6	25%
2024-T3	40	0.02	Cyl	13000	6	10%
2024-T3	40	0.02	Flat	13000	6	Nf
2024-T3	40	0.02	Flat	13000	6	50%
2024-T3	40	0.02	Flat	13000	6	25%
2024-T3	40	0.02	Flat	13000	6	10%
		Total Coupons			96	

Table 5 Test matrix for Low Kt fretting fatigue. Note: it may be possible to eliminate one of the punch geometries. If so, the test matrix could be reduced from 96 to 60 coupons by eliminating the second punch geometry for all of the interrupted tests.

Decision point will be based on statistical difference in N_f tests between punch geometries.

2.3.2.3 Fretting Fatigue Behavior in High Kt Coupons

As we move into more complex coupons, the number of variables can be reduced. For this sub-series of tasks, the goal is to predict (using information from the low Kt experiments) the locations where coupons will fail when fretting contact stresses interact with the more complex stress field associated with a hole. Coupon geometry will be a 2 inch wide, bare 2024-T3 sheet, 0.063 inch thick, with a single 3/16 inch diameter straight-through hole.

The High Kt test coupon is schematically shown in Figure 20, and will use coupon and fretting pad designs as indicated. Most fretting tests documented in the literature use a flat or cylindrical pad fretting on a $K_t=1$ (no notch or hole), therefore these element tests will accomplish two goals: 1) fretting at a hole, representative of a hole in a lap joint and 2) fretting with alternative fretting pad geometries. The analytical methods of **Sections 2.3.2.1** and **2.3.2.2** will be correlated with these results, to determine if the finite element calculated stresses can be used to successfully correlate fretting at holes.

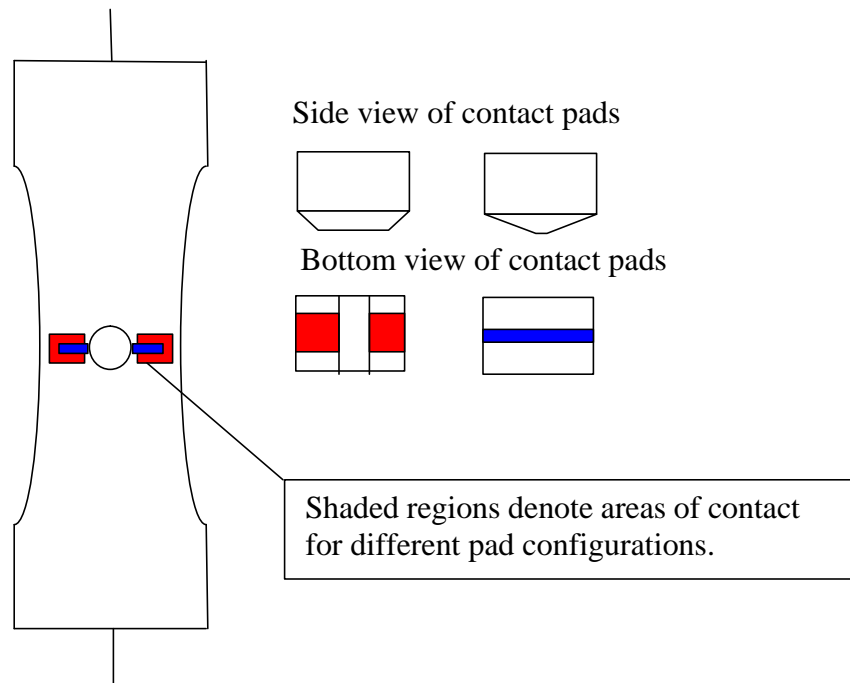


Figure 20 Hole Configuration to Be Tested. Two Geometries of Fretting Pads Will Be Tested, and Will Be Similar to Those Shown Schematically.

For this experimental series, the test variables are:

- Alternating Fatigue Stress
- Normal Pressure Level
- Area of Fretting Pad Contact Relative to Hole Location

The stress ratios, test frequency, and environment are all the same as in the low Kt matrices. The alternating stress levels will be adjusted based on the Kt of the hole, which will be

determined by finite elements. For now, assuming a K_t of 3.2, the two alternating fatigue stresses (remote) would be 9.375 ksi and 12.5 ksi.

The normal pressure levels would be the same as used for the low K_t fretting fatigue tests.

The size of the contact pad will be variable, one large and one small, as shown in Figure x. This will change the location of the maximum stress interaction between K_t of the hole and fretting contact. Analytical tools will be exercised in an attempt to not only predict cycles to failure, but to predict location of failure, too. Table 6 shows the Hi K_t fretting fatigue matrix.

Response parameters to be measured will be cycles to visual crack detection (VCD) and location of the failure. Fractography and metallography will be used to study and record crack nucleation sites, surface damage, and crack morphologies. The specimen will not be allowed to completely fracture, as all the extra crack growth produces detrimental damage to the fracture face while adding few additional cycles to the fatigue test.

Material	Stress Level (max ksi)	Stress Ratio	Punch Geometry	Normal Pressure (psi)	Replicates	Interrupt Level
2024-T3	30	0.02	Large	8000	4	Visual Crack Detection (VCD)
2024-T3	40	0.02	Large	8000	4	VCD
2024-T3	40	0.02	Small	8000	4	VCD
2024-T3	30	0.02	Large	13000	4	VCD
2024-T3	40	0.02	Large	13000	4	VCD
2024-T3	40	0.02	Small	13000	4	VCD
				Total Coupons	24	

Table 6 High K_t Test Matrix for Fretting Fatigue

2.3.2.4 Single Rivet Lap Joint (SRLJ) Fatigue Tests

To raise the level of realism, complex coupon tests will be followed by simple element tests in the form of a single rivet lap joint, Figure 14. Fretting damage will now be generated by faying surface contact in the joint rather than by a fretting pad. Rivet squeeze force (or fastener torque) will be carefully controlled to simulate contact pressures in the fretting pad experiments. Two different squeeze forces will be used, along with two different alternating stresses. Protruding head rivets/fasteners are recommended; the additional complexity introduced by countersunk holes is avoided, and fretting will then be significant only at the faying surfaces or between the head/tail and sheet. Measured responses will be cycles to visual crack detection and failure locations. It is desirable to stop the test upon crack detection, as continued growth will only damage the fracture surfaces and will do little to

further illustrate life prediction capability. Most of the life will already have been consumed by the time a faying crack becomes a through crack.

Analytical methods of the HLPM will be used to predict the fatigue life (to break through) and failure locations. Fractography will be conducted to thoroughly document the fracture behavior.

A simple test matrix follows in Table 7. Note if the test matrix as specified in Table 5 above can be reduced based upon the findings in test results, the matrix in Table 7 will be increased.

Material	Stress Level (max ksi)	Stress Ratio	Squeeze Force (lbs)	Replicates	Interrupt Level
2024-T3	9.375	0.02	Variable	4	Visual crack detection (VCD)
2024-T3	9.375	0.02	Variable	4	VCD
2024-T3	12.5	0.02	Variable	4	VCD
2024-T3	12.5	0.02	Variable	4	VCD
			Total Coupons	16	

Table 7 Test Matrix for Single Rivet Lap Joint Experiments.

2.3.2.5 Multiple Rivet Lap Joint (MRLJ) Fatigue Tests

The above sections describe the minimum elements needed in a fundamental test plan to address prediction model needs. Validation and verification to expand the applications would continue to build on the testing building block approach of Figure 19. For instance, additional complexity can be introduced by testing the multiple rivet lap joint (MRLJ) configuration shown in Figure 18. The MRLJs can be tested using the same procedures outlined the in SRLJ tests in **Section 2.3.2.4** above. The MRLJ configuration allows many more possibilities than the SRLJ. For instance, more variations on magnitude and location of various squeeze force levels can be made: (1) all the fasteners installed with the same squeeze force, (2) top and bottom rows installed with high squeeze force, and middle row installed with low squeeze force, (3) top and bottom rows installed with low squeeze force, and middle row installed with high squeeze force, (4) top and middle rows installed with high (or low) squeeze force, and bottom row installed with low (or high) squeeze force, (5) top row installed with high (or low) squeeze force, and middle and bottom rows installed with low (or high) squeeze force. Variations by column can be introduced as well. The level and extend of follow-on test programs should be based upon the structural application of concern and utilize the advances made in the assessment methods to determine the sensitive parameters that should be pursued.

2.4 Task IV: Fretting Fatigue Model Integration

One of the principal goals of this Phase I project was to demonstrate that the one or two candidate fretting fatigue analytical approaches that were identified early in Phase I could be integrated into an existing structural integrity framework, thereby demonstrating feasibility of our approach. The existing structural integrity framework, the Holistic Life Prediction Methodology, has previously been documented in open literature (72) and described in Section 1.2 above. This framework allows introduction of many degradation mechanisms into structural life predictions; including, our Phase I efforts have shown, fretting damage mechanisms. For Phase I, only the Hattori fracture mechanics based model was integrated into the framework, and correlated with test data described by Hoepfner and Goss (66). Any integration must be validated; therefore a technology development plan to validate methods is described.

This section summarizes investigations into two major thrusts of technology development: integration and validation. Integration of the analytical methods into an existing structural integrity framework is needed to facilitate transition of technology to the potential users. Also described is a technology development plan to validate methods with a four-pronged approach: 1) correlation of analytical methods with experimental test data, 2) comparison of Stress Intensity Factors (SIFs) computed with finite element software against the Rooke and Jones methods summarized in Equations (4) and (5) in **Section 2.2.1** above, 3) correlation of finite element method simulations and normal contact pressures measured with the Fuji film technique, and 4) finite element method simulations of the complex, three-dimensional states of stress in the Single Rivet Lap Joint (SRLJ), with special emphasis on friction effects.

2.4.1 Correlation

Correlation of the analytical methods with experimental data is essential to validation of the methods. This section describes a preliminary correlation of the Hattori analytical model as integrated with the Holistic Life Prediction Methodology with experimental test data.

As an example of the first validation activity, the Hattori closed-form solution that was implemented into the Holistic Life Prediction Methodology (the software that implements this methodology is called 'ECLIPSE') was exercised in an attempt to determine the model robustness. Contact pressure simulations for two types of loading have been incorporated into the ECLIPSE code. The graphical user interface (GUI) for the flat punch contact loading case is shown in Figure 21.

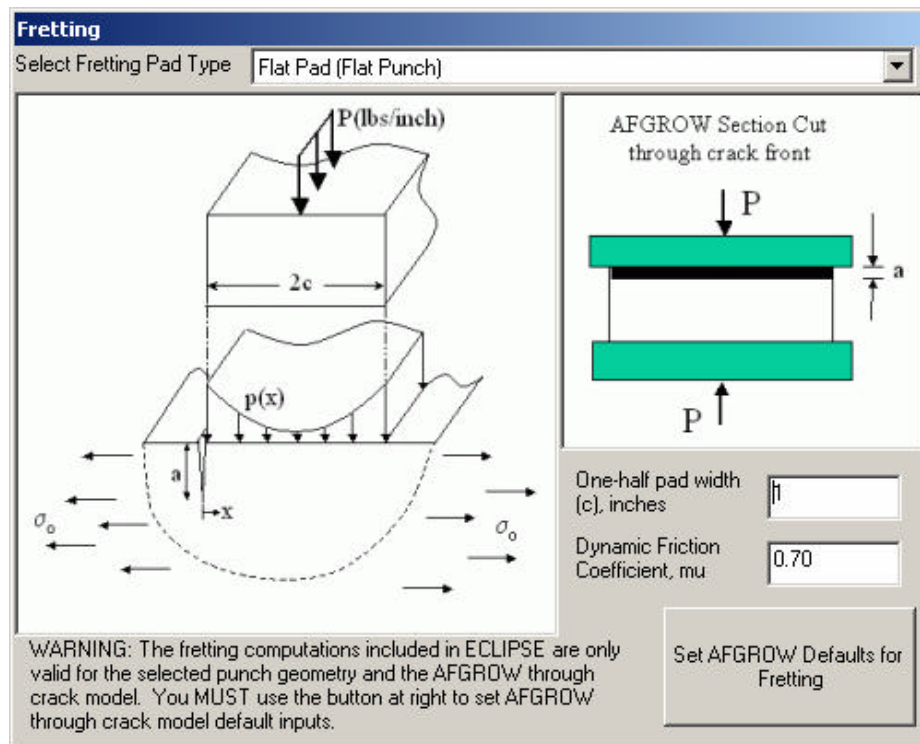


Figure 21 Flat Punch Model in ECLIPSE Implements Hattori's Model and Can be Easily Extended to Incorporate 'Crack Analogue'.

The fretting equations for K_I as a function of contact normal and tangential tractions have been directly combined with the internally computed K_I for this specific punch geometry. The input parameters include the punch width and the dynamic friction coefficient, the latter determining the percent contribution of the tangential traction (normal to the $p(x)$ function shown). As this is the flat punch case, the stick-slip boundary is assumed to begin at the punch corner. The coefficient of friction (m) is simply a multiplier on the normal force, representing the fact that the force Q is equal to $m * P$. The shear function distribution $q(x)$ is also modeled as being equal to $m * p(x)$.

The holistic framework is ideal for quantifying the contributions of fretting, fatigue, and other mechanisms of material damage in an integrated scheme that considers possible interactions. By using numerical integration and sufficiently small time steps, the effects of fretting on fatigue crack nucleation are captured as well as the effects of cyclic crack nucleation/growth on the fretting component of the discontinuity state progression.

Figure 22 shows an example of holistic, time-based inputs to the fretting fatigue model. The holistic framework gives the analyst the power to represent time-dependent fretting load changes as displayed in Figure 22 (fretting load applied for 10 years (2000 fatigue cycles) then no fretting load applied after that).

The screenshot shows the ECLIPSE software window with a menu bar (File, Tools, Guidelines, About) and a main panel titled 'Time Dependent Inputs'. On the left, there are four buttons: 'Thickness Loss', 'Topography ID', 'Direct Pitting', and 'Fretting Load' (which is highlighted). The main panel contains a table with two columns: 'Time (years)' and 'Fretting Load (kips/inch)'. The table has four rows of data. Below the table are 'Plot' and 'Help' buttons. At the bottom left, there are two input fields: 'Integration Interval (years). Small values are more accurate but run slowly.' with a value of '1', and 'Cycles per Integration Interval' with a value of '200'. On the right side, there is a 'Set Defaults for:' dropdown menu set to 'Lap Splice', an 'Edit (View AFGROW)' button, a 'Residual Strength R'qmt (Pxx)' input field with a value of '1.5', a 'Run Age Degradation Analysis' button, and a 'Quit' button.

Time (years)	Fretting Load (kips/inch)
0	4
10	4
10.001	0
100	0

Figure 22 Time-Dependent Fretting Inputs to ECLIPSE.

Results of the implementation of the Hattori model into ECLIPSE are captured by traditional crack growth ' a vs. N ' curves. Figure 23 shows the ECLIPSE result of an analysis with fatigue loads and fretting loads. The last column of Figure 23 displays the contribution of the fretting load to the total stress intensity at the current time step, Fretting K / (Fretting K + Cyclic Fatigue K).

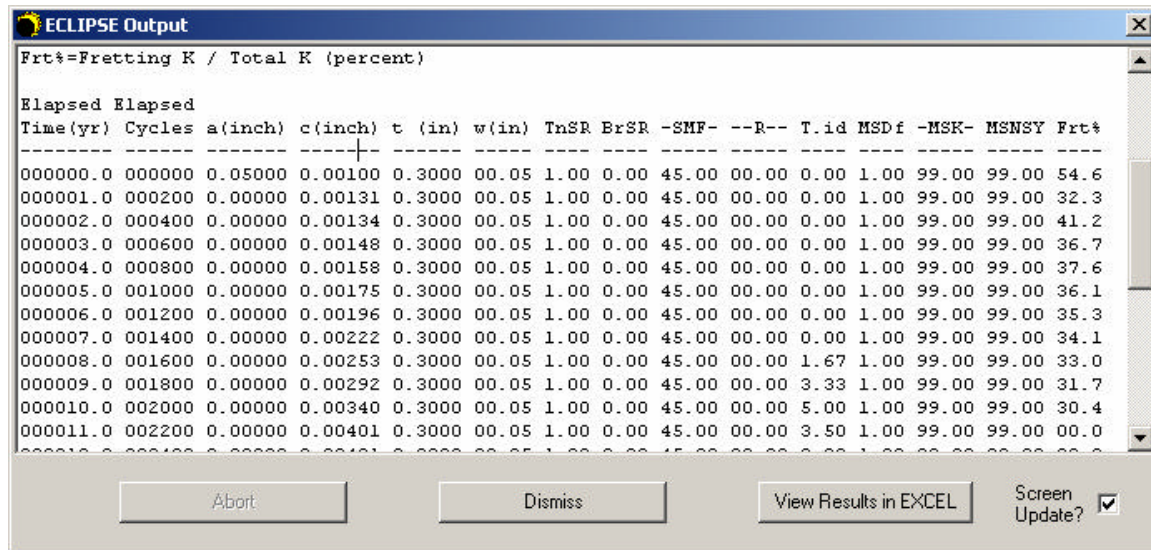


Figure 23 ECLIPSE Output Including Fretting Contribution to Holistic Analysis.

The 7075-T6 pristine and fretting stress-life data were extracted from a Naval Research report by Hoepfner and Goss (66). The maximum applied stress in the fretted coupon was varied from 15 to 60 ksi, stress ratio was fixed to $R=1.0$. The normal stress averaged over the fretting pad was 3 ksi. The average frictional (shear) stress on the fretting pad was not recorded. The fretted coupons were 0.05" thick. While some coupons were tested with "partial fretting", that is, the fretting pad was present for a percentage of overall test coupon life, the correlations here examine only the 'fully fretted' coupons, that is, coupons that were fretted from the initial cycle to final cycle of life. Several assumptions had to be made to apply this fretting model to this specific data set, the details of which are documented below. Due to the extreme uncertainties of crack growth data in the 'short crack' regime (considered here as da/dN less than $1e-8$ inches/cycle), two material models were used in an attempt to see the effect on the fretting model correlation. The first material model (model A) was a data set that had been previously used for other 7075-T6 fatigue test correlations. Model A has short crack behavior built-in, though the crack growth rates are not as fast as the short crack da/dN rates that emerged for 2024-T3 during AGARD roundtable experiments in the 1980's. The correlation of this fretting data using Model A is shown in Figure 24 below. In light of the AGARD work and the unavailability of short crack data for 7075-T6, an alternate material model (designated as model B) was also examined in hopes that one of the two models would provide better correlation, Figure 25. Model A has moderate short-crack behavior, model B has the same long-crack growth rates as model A but much faster, or severe, short-crack growth rates than Model A. Note that the IDS was calibrated separately for each material Model by tuning to the pristine data points in Figure 24 and Figure 25.

For the correlation method presented in this report, several assumptions were made in order to perform the correlation.

- A part-through surface crack EIFS value ($a=c$, $c=1/2$ of the surface crack length) that best fit the pristine test specimen curve was calculated for each material model, A and B, in order to tune the model to the pristine specimen results. The EIFS value was calculated by averaging the EIFS for all the pristine data points. The EIFS for Model A was 0.0015 inch, the EIFS for Model B was 0.0010 inch. These two EIFS values were used during the calculation of the fretting predictions for material models A and B.
- The fretting pad used in the experiment was a square pad that applied normal pressure in the middle of the coupon faces. However, the known solution for a flat pad assumes that the flat pad extends all the way across the width of the test specimen. Assumption: the square pad behaves identically to the flat pad. In reality, the square pad is probably more severe than the flat pad due to the effects of the pad corners.
- The known flat pad solution is intended for use on through cracks only. The final correlation documented in the Phase 1 final report utilized part-through cracks. Assumption: part-through cracks are affected by fretting amplifications identically to through cracks.
- The ECLIPSE code was modified such that the fretting stress intensity amplification would be applied to both the a and c dimensions of the part-through crack. This was done by calculating the fretting K using the flat pad-through crack method, assuming that $a=c$, then computing an equivalent beta correction factor that would produce the proper delta in the stress intensity that is due to the fretting contribution. This beta correction factor was applied to both the a and the c dimensions of the part-through crack. This calculation was performed at each ECLIPSE time/cyclic step increment (integration interval).
- A dynamic friction coefficient of zero was used during the correlation, so that no shearing effects on the solution were considered. The shearing force term in the closed-form flat pad model alternates sign depending on whether the specimen is being loaded or unloaded during the fatigue cycle, so the assumption is that the shearing forces that contribute to fretting will cancel out (i.e. shearing forces are detrimental to fatigue life during the loading portion of the load cycle, and beneficial during the unloading portion).

In summary, Model A appears to pick up the threshold behavior of the pristine specimens better, where as Model B correlates the low stress fretting data better. The results of these correlations indicate that a modification to the closed-form Hattori model may be necessary to produce fretting life degradations that will be more robust across all of the stress levels shown in Figure 24 and Figure 25.

2.4.2 Validation of Rooke and Jones Methods

Finite element method software will be used to determine the accuracy of the Stress Intensity Factors that are computed using the Rooke and Jones methods summarized in Equations (4) and (5) in **Section 2.2.1** above. Briefly, the Rooke and Jones methods use estimates of the

normal and shear contact tractions caused by the fretting of the test coupon and the fretting pad to calculate Model I Stress Intensity Factors (SIFs), K_I for an edge crack perpendicular to the surface that the fretting pad contacts. The p -version finite element method software StressCheck[®] (ESRD, Inc., St. Louis, Missouri) will be used to validate the Rooke and Jones methods for two contact geometries: flat pad and cylindrical pad contacting $K_t=1$ test coupons. Normal and shear contact tractions, fretting pad width, crack length, and test coupon width will be varied. A representative flat pad mesh is shown in Figure 26 below.

2.4.3 Validation of Normal Contact Pressure Simulations

Realistic simulations of the normal and shear contact tractions with the finite element method are difficult even for simple fretting pad-coupon geometry. In addition, accuracy and reliability in the finite element simulations are challenging because of the nonlinearities in the contact problem. The Fuji film method described in **Section 2.3.1.2** above can be quite useful in this regard. Recall that Fuji film method uses color contours in film inserted in between two contact bodies to measure the normal contact pressure. The finite element method software Marc (MSC Software Corp., Redwood, California), which has specialized nonlinear and contact mechanics capabilities, will be used to simulate the contact of two thin plates that have been riveted together with a force controlled rivet machine. Rivet force and plate thickness will be varied in the experiments and the finite element simulations.

2.4.4 Single Rivet Lap Joint (SRLJ) Simulations

These simulations are not ‘validations’ in the usual sense: there simply is no known method to accurately measure the complex, three-dimensional states of stress in the Single Rivet Lap Joint (SRLJ). Nevertheless, finite element method simulations of the stresses in SRLJ will be attempted, with special emphasis on frictional effects. The goal of this analysis is to gain insight into the complex states of stress in lap joints and use this insight to improve the analytical correlations with the SRLJ fatigue test results.

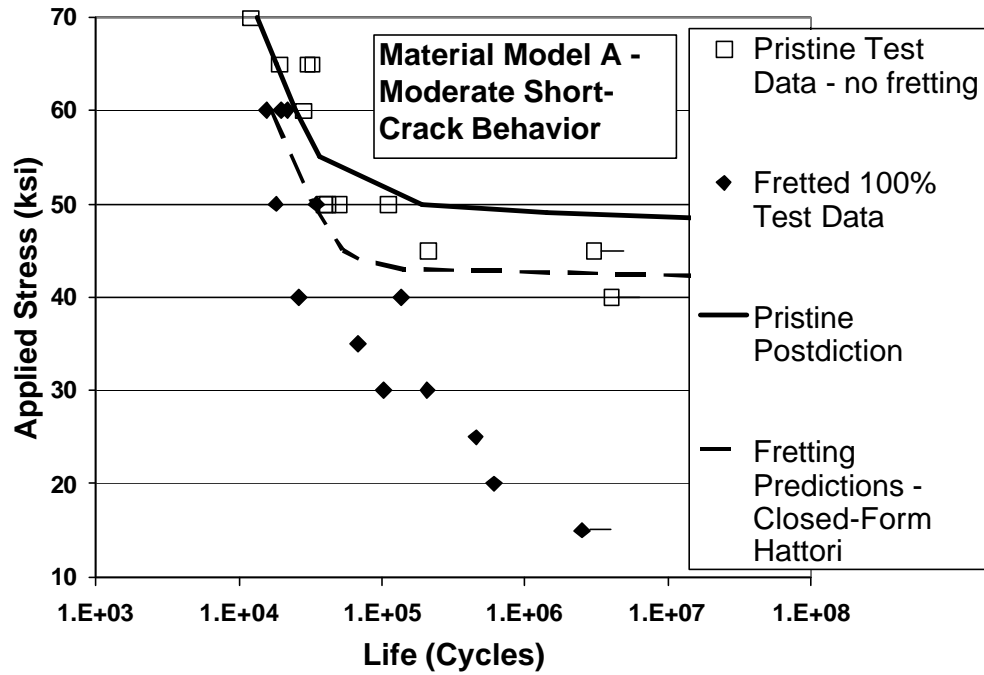


Figure 24 Hattori Closed-Form Fretting Model Behavior, Material Model A.

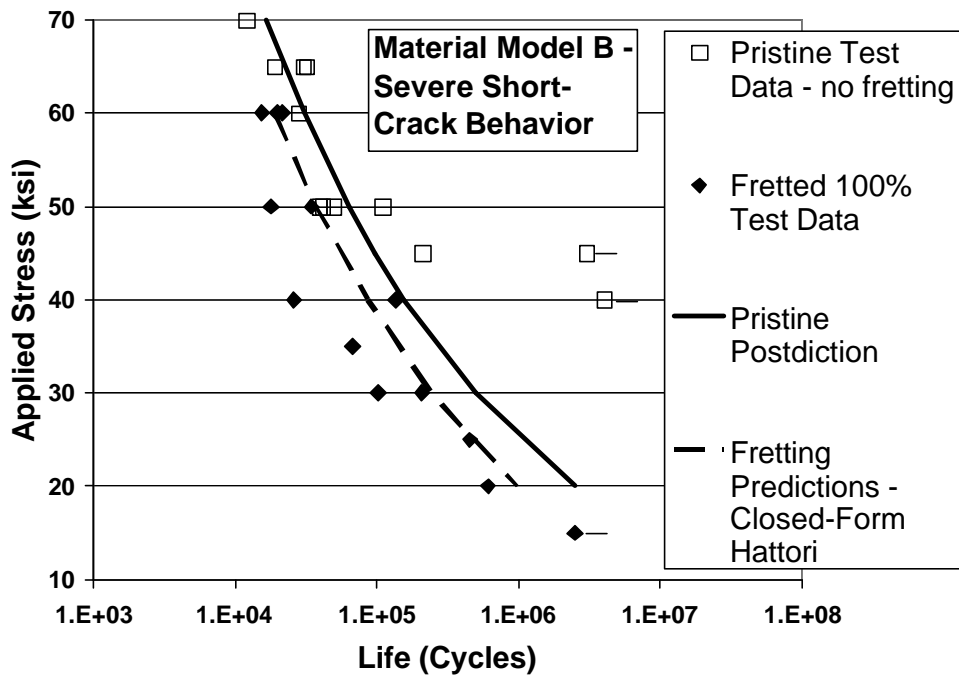


Figure 25 Hattori Closed-Form Fretting Model Behavior, Material Model B.

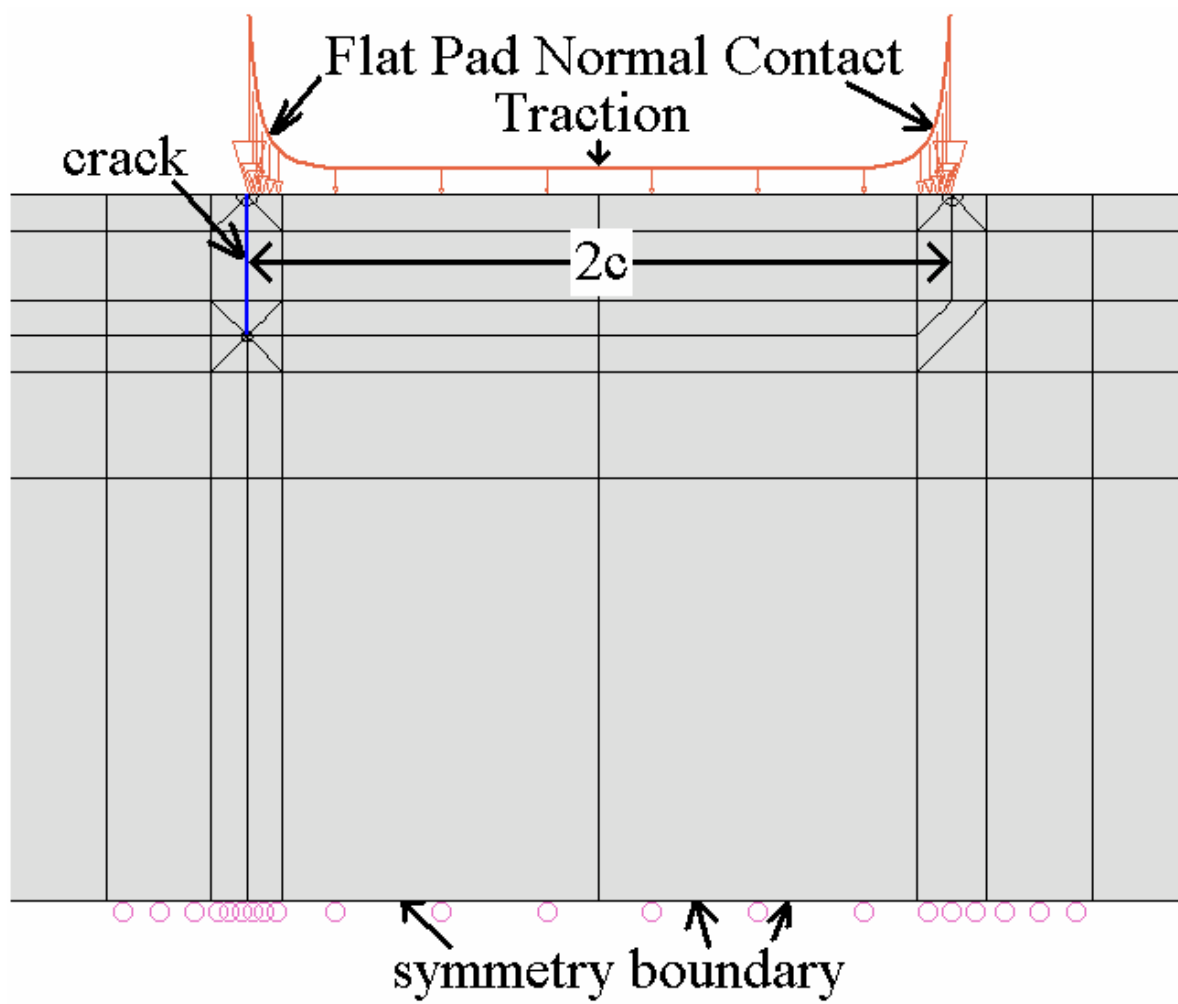


Figure 26 StressCheck Finite Element Mesh Used to Simulate Flat Pad Contact.

3.0 CONCLUSIONS

In summary, research documented in this report indicates:

- The two candidate analytical prediction methods (Hattori Method and Crack Analogue) are mature enough to allow introduction of fretting fatigue into an existing structural integrity framework; one of the candidate analytical predictive models, the Hattori Model, has been integrated into an existing structural integrity framework (and assessment analytical tool).
- The analytical results correlated with experimental data trends of fretting fatigue life of simple coupons. While correlation results so far have not been perfect or even good, the correlation described in this report is nevertheless encouraging as they indicate the simulation of the predominant effects of the fretting test results. Given that the Crack Analogue approach is fracture mechanics-based, similar to the Hattori Model, there should be little trouble integrating the Crack Analogue method into the same life prediction methodology used with the Hattori Model. In addition,
- A demonstrated assessment analytical tool, ECLIPSE, readily engulfs both of the concepts. The continued building and expansion of the models as supplemented by empirical data enable the benefits of being able to assess the fretting effects on fatigue to be applied to meet structural maintenance objectives.

4.0 REFERENCES

- (1) Mitchell, John S. (1998) "Five to Ten Year Vision for CBM", presented at the ATP Fall Meeting—Condition-Based Maintenance Workshop, Atlanta, Georgia, November 17, 1998.
- (2) Davis, J.R. [Editor] (1999) Metals Handbook: Desk Edition, ASM International Handbook Committee.
- (3) Waterhouse, R.B. (1972) Fretting Corrosion, Pergamon Press, USA.
- (4) Specialist Meeting on Fretting in Aircraft Systems (1974) NATO-AGARD Conference Proceedings No. 161, AGARD.
- (5) *Control of Fretting Fatigue* (1977) Report of the Committee on Control of Fretting-Initiated Fatigue, NMAB, NRC, Publication NMAB-33, National Academy of Sciences, Washington, D.C.
- (6) Waterhouse, R.B. [Editor] (1981) Fretting Fatigue, Applied Science Publishers, UK.
- (7) Attia/Waterhouse [Editors] (1992) Standardization of Fretting Fatigue Test Methods and Equipment, ASTM STP 1159, ASTM, Philadelphia, PA.
- (8) Waterhouse/Lindley [Editors] (1994), Fretting Fatigue, ESIS Publication 18, Mechanical Engineering Publications Ltd., London, England.
- (9) Hoepfner, D. W. (1992) "Mechanisms of Fretting Fatigue and Their Impact on Test Method Development", Keynote paper, *Standardization of Fretting Fatigue Test Methods and Equipment, ASTM STP 1159*, M. Helmi Attia and R.B. Waterhouse, Eds., American Society for Testing and Materials, Philadelphia, PA, pp 23-31.
- (10) Hoepfner, D. W. (1994) "Mechanisms of Fretting Fatigue", Keynote paper, *Fretting Fatigue*, ESIS 18, Edited by R. B. Waterhouse and T.C. Lindley, Mechanical Engineering Publications, London, 3-19.
- (11) Hoepfner, D. W. (2001) "Fretting Fatigue Life Prediction: Past, Present and Future", Keynote paper, Presented at the Third International Symposium on Fretting Fatigue, Nagoaka, Japan. (In review for publication by ASTM).
- (12) Nishioka, K., Nishimura, S., and Hirakawa, K. (1968) "Fundamental Investigation of Fretting Fatigue - Part 1, On the Relative Slip Amplitude of Press-fitted Axle Assemblies", *Bulletin of JSME*, **11**, No 45, 437-445.
- (13) Nishioka, K., and Hirakawa, K. (1969) "Fundamental Investigation of Fretting Fatigue - Part 2, Fretting Fatigue Testing Machine and Some Test Results", *Bulletin of JSME*, **12**, No 50, 180-187.
- (14) Nishioka, K., and Hirakawa, K. (1969) "Fundamental Investigation of Fretting Fatigue - Part 3, Some Phenomena and Mechanisms of Surface Cracks", *Bulletin of JSME*, **12**, No 51, 397-407.
- (15) Nishioka, K., and Hirakawa, K. (1969) "Fundamental Investigation of Fretting Fatigue - Part 4, The Effect of Mean Stress", *Bulletin of JSME*, **12**, No 51, 408-414.
- (16) Nishioka, K., and Hirakawa, K. (1969) "Fundamental Investigation of Fretting Fatigue - Part 5, The Effect of Relative Slip Amplitude", *Bulletin of JSME*, **12**, No 52, 692-697.
- (17) Nishioka, K., and Hirakawa, K. (1972) "Fundamental Investigation of Fretting Fatigue - Part 6, Effects of Contact Pressure and Hardness of Materials", *Bulletin of JSME*, **15**, No 80, 135-144.
- (18) Endo, K., Goto, H., and Nakamura, T. (1969) "Effects of Cycle Frequency on Fretting Fatigue Life of Carbon Steel", *Bulletin of JSME*, **12**, No 54, 1300-1308.
- (19) Waterhouse, R. B. (1972) "The Effect of Fretting Corrosion in Fatigue Crack Initiation", *Corrosion Fatigue: Chemistry, Mechanics, and Microstructure*, NACE-2 conference, June

- 14-18, 1971, at The University of Connecticut, Storrs, Connecticut; Published by NACE (National Association of Corrosion Engineers), Houston, 608-616.
- (20) Hoepfner, D. W., and Goss, G. G. (1972) "Research on the Mechanism of Fretting Fatigue", *Corrosion Fatigue: Chemistry, Mechanics, and Microstructure*, NACE-2 conference, June 14-18, 1971, at The University of Connecticut, Storrs, Connecticut; Published by NACE (National Association of Corrosion Engineers), Houston, 617-626.
- (21) Endo, K., and Goto, H. (1976) "Initiation and Propagation of Fretting Fatigue Cracks", *Wear*, **38**, 311-324.
- (22) Hoepfner, D.W. (1977) "Comments on Initiation and Propagation of Fretting Fatigue Cracks" (letter to the editor), *Wear*, **43**, 267-270.
- (23) Edwards, P. R. (1981) "The Application of Fracture Mechanics to Predicting Fretting Fatigue", *Fretting Fatigue*, R.B. Waterhouse (Editor), Applied Science Publishers, Ltd., Essex, England, 67-97.
- (24) Prost-Domasky, Scott A., Brooks, Craig L., and Honeycutt, Kyle T. (2000) "The Application of p -version Finite Element Methods to Fracture-dominated Problems Encountered in Engineering Practice", *Proceedings of p- and hp-Finite Element Methods: Mathematics and Engineering Practice Conference (p-FEM2000)*, St. Louis, MO. To appear in *Computer & Mathematics with Applications* (refereed), 2003.
- (25) Hoepfner, D. W., Mann, D., Weekes, J. (1981) "Fracture Mechanics Based Modeling of the Corrosion Fatigue Process", *Specialist Meeting on Corrosion Fatigue NATO-AGARD, 52nd Meeting of the Structures and Materials Panel, 04:05-10*, Çesme, Turkey.
- (26) Berthier, Y., Godet, M., and Vincent, L. (1988) "Fretting Wear and Fatigue: Initiations, Mechanisms, and Prevention", *Mec. Matel. Elect.*, 20-26.
- (27) Berthier, Y., Colombie, Ch., Vincent, L., and Godet, M., 1988, "Fretting Wear Mechanisms and Their Effects on Fretting Fatigue," *Trans. Of the ASME, Journal of Tribology*, **110**, 517-524.
- (28) Petiot, C., Vincent, L., Dang Van, K., Maouche, N., Foulquier, J., and Journet, B., 1995, "An Analysis of Fretting-Fatigue Failure Combined with Numerical Calculations to Predict Crack Nucleation," *Wear*, **181-183**, 101-111.
- (29) Lamacq, V., Dubourg, M.C., and Vincent, L. (1996) "Crack Path Prediction Under Fretting Fatigue—A Theoretical and Experimental Approach," *Trans. of the ASME, Journal of Tribology*, **118**, 11-720.
- (30) Fouvry, Siegfried, Kapsa, Philippe and Vincent, Leo (1996) "Quantification of Fretting Damage," *Wear*, **200**, 186-205.
- (31) Zhou, Z.R., and Vincent, L. (1997) "Cracking Induced by Fretting of Aluminum Alloys," *Trans. of the ASME, Journal of Tribology*, **119**, 36-42.
- (32) Fouvry, S., Kapsa, P. and Vincent, L. (2000) "Fretting-Wear and Fretting-Fatigue: Relation Through a Mapping Concept," *Fretting Fatigue: Current Technology and Practices, ASTM STP 1367*, 49-64.
- (33) Fouvry, S., Kapsa, P. and Vincent, L., (2000) "A Multiaxial Fatigue Analysis of Fretting Contact Taking Into Account the Size Effect," *Fretting Fatigue: Current Technology and Practices, ASTM STP 1367*, 167-182.
- (34) Dang Van, K. and Maitournam, M.H. (2000) "On a New Methodology for Quantitative Modeling of Fretting Fatigue," *Fretting Fatigue: Current Technology and Practices, ASTM STP 1367*, 538-552.

- (35) Vincent, L., Godet, M., and Berthier, Y. (1994) Rapport final, Contract “Programme Fretting—Fatigue”, No. 9196030004717586, 178 pages.
- (36) Hattori, T., Nakamura, M., Sakata, H., and Watanabe, T. (1988) “Fretting Fatigue Analysis using Fracture Mechanics”, *Japan Society of Mechanical Engineers International Journal—Series I*, **31**, 100-107.
- (37) Hattori, T., Nakamura, M., Watanabe, T. and Okuno, S. (1999) “Standardization of Fretting Fatigue Test Considering on Stress Distributions Near a Contact Edge”, in *Computational Methods in Contact Mechanics IV*, 421-30.
- (38) Hattori, T., Kawai, S., Okamoto, N. and Sonobe, T., (1981) “Torsional Fatigue Strength of a Shrink Fitted Shaft,” *Bulletin of the JSME*, **24**, No. 197, 327-344.
- (39) Hattori, T., Nakamura, M., Sakata, H., and Watanabe, T. (1988) “Fretting Fatigue Analysis Using Fracture Mechanics,” *JSME International Journal, Series I*, **31**, No. 1, 100-107.
- (40) Hattori, T. and Sakata, S. (1988) “A Stress Singularity Parameter Approach for Evaluating Adhesive and Fretting Strength,” in *Advances in Adhesively Bonded Joints-MD-Vol. 6*, 43-50
- (41) Hattori, T. Nakamura, M. and Ishizuka, T. (1992) “Fretting Fatigue Analysis of Strength Improvement Models with Grooving or Knurling on a Contact Surface,” in *Standardization of Fretting Fatigue Test Methods and Equipment, ASTM STP 1159*, 101-114.
- (42) Hattori, T. and Nakamura, M. (1994) “Fretting Fatigue Evaluation Using Stress Singularity Parameters at Contact Edges,” *Fretting Fatigue, ESIS 18*, Mechanical Engineering Publications London, 453-460
- (43) Hattori, T. (1994) “Fretting Fatigue Problems in Structural Design,” *Fretting Fatigue, ESIS 18*, Mechanical Engineering Publications, London, 437-451.
- (44) Hattori, T., Nakamura, M., and Ishizuka, T. (1995) “Fretting Fatigue Evaluation Using Stress Singularity Parameters,” *ISME Yokohama*, 564-567.
- (45) Hattori, T., Nakamura, M., Watanabe, T., and Okuno, S. (1999) “Standardization of Fretting Fatigue Test Considering on Stress Distributions Near a Contact Edge,” *Computational Methods in Contact Mechanics*, 421-430.
- (46) Hattori, T., and Watanabe, T. (2000) “Fracture Mechanics Analyses of Fretting Fatigue Cracks Considering Propagation Directions,” *Proc. Eur. Conf. EUROMAT 2000 on Advances in Mechanical Behavior, Plasticity & Damage*, 1015-1020.
- (47) Hattori, T., Nakamura, M., and Watanabe, T. (2000) “A New Approach to the Prediction of the Fretting Fatigue Life that Considers the Shifting of the Contact Edge by Wear,” *Fretting Fatigue: Current Technology and Practices, ASTM STP 1367*, 19-30.
- (48) Hattori, T., Nakamura, M., and Watanabe, T. (2001) “Fretting Fatigue Life Simulation using Stress Singularity Parameters and Fracture Mechanics,” *Materials Science Research International, STP-I*, 208-215.
- (49) Hattori, T., Nakamura, M., and Watanabe, T. (2002) “Improvement of Fretting Fatigue Strength by Using Stress-Release Slits,” *Fretting Fatigue: Experimental and Analytical Results, ASTM STP 1425*.
- (50) Giannakopoulos, A.E., Lindley, T.C., and Suresh, S. (1998) “Aspects of Equivalence Between Contact Mechanics and Fracture Mechanics: Theoretical Connections and a Life-Prediction Methodology for Fretting-Fatigue”, *Acta Materialia*, **46**, No. 9, 2955-2968.
- (51) Giannakopoulos, A.E., Lindley, T.C., Suresh, S., and Chenut, C. (2000) “Similarities of Stress Concentrations in Contact at Round Punches and Fatigue at Notches: Implications to

- Fretting Fatigue Crack Initiation”, *Fatigue and Fracture of Engineering Materials in Structures*, **23**, 561-571.
- (52) Matika, T.E., Shell, E., and Nicalou, P.D. (1999) “Characterization of Fretting Damage Using Nondestructive Approaches”, *Proceedings of the Nondestructive Evaluation of Aging Materials and Composites III*, **3585**, Newport Beach, Virginia, 2-10.
- (53) Frantziskonis, G.N., Shell, E., Woo, J., Matikas, T.E., and Nicolau (1999) “Wavelet Analysis of Fretting Experimental Data”, *Proceedings of the Nondestructive Evaluation of Aging Materials and Composites III*, **3585**, Newport Beach, Virginia, 11-27.
- (54) Kramb, Victoria, Shell, Eric, Hoying, Jody, Simon, Laura, and Meyendorf (2001) “Applicability of White Light Scanning Interferometry for High Resolution Characterisation of Surface Defects”, *Proceedings of the Nondestructive Evaluation of Aging Materials and Composites V*, **4336**, Newport Beach, Virginia, 135-145.
- (55) Meyendorf, Norbert (2001) “Development of Enabling Methodologies for Detection and Characterization of Early Stages of Damage in Aerospace Materials”, Final Report for DARPA Multi-University Interdisciplinary Research Initiative (MURI) conducted under the Air Force Office of Scientific Research (AFOSR).
- (56) Ishida, Yuji, and Chiba, Norimasa (1999) “Contact Surface Damage Evaluation by Infrared Thermography”, *AIP Conference*, **497**, 355-360.
- (57) Shatat, A., Atherton, David L. (1997) “Remote Field Eddy Current Inspection of Support Plate Fretting Wear”, *Materials Evaluation*, 55, No. 4, 361-366.
- (58) Brooks, C.L. and Simpson, D. (1998) “Integrating Real Time Age Degradation into the Structural Integrity Process” *Proceedings of NATO RTO’s Workshop 2 on Fatigue in the Presence of Corrosion*, Corfu, Greece.
- (59) Brooks, C., Peeler, D., Honeycutt, K.H., and Prost-Domasky, S. (1999) “Predictive Modeling for Corrosion Management: Modeling Fundamentals”, *Proceedings of the Third Joint NASA/FAA/DoD Conference on Aging Aircraft*, Albuquerque, New Mexico.
- (60) Brooks, C.L., Prost-Domasky, S. and Honeycutt, K. (1998) “Determining the Initial Quality State for Materials”, *Proceedings of the 1998 USAF Aircraft Structural Integrity Program Conference*, San Antonio, Texas.
- (61) Vingsbo, O. and Soederberg, S., 1988 “On Fretting Maps”, *Wear*, **126**, 131-147.
- (62) Hills, D.A., Nowell, D. and O’Connor, J.J., (1988) “On the Mechanics of Fretting Wear”, *Wear*, **125**, 129-146.
- (63) Rooke, D.P. and Jones, D.A. (1979) “Stress Intensity Factors in Fretting Fatigue”, *J. Strain Analysis*, **14**, No. 1, 1-6.
- (64) Archard, J.F. (1953) “Contact and Rubbing of Flat Surfaces”, *J. Applied Physics*, **24**, No. 8, 981-988.
- (65) Isida, M. (1979) “Tension of a Half Plane Containing Array Cracks, Branched Cracks, and Cracks Emanating from Sharp Notches”, *Transactions of the Japanese Society of Mechanical Engineers Series A*, **45**, 306-317.
- (66) Hoepfner, David W. and Goss, Gary L. (1972) “The Effect of Fretting Damage on the Behavior of Metals – Technical Report 1,” *Office of Naval Research, Contract N00014-71-C-0299*, 23.
- (67) Pearson, S. (1975) “Initiation of Fatigue Cracks in Commercial Aluminum Alloys and the Subsequent Propagation of Very Short Cracks,” *Engineering Fracture Mechanics*, **7**, 235-247.

- (68) Bartolo, E.A. and Hillberry, B.M. (1998) "Effects of Constituent Particle Clusters on Fatigue Behavior of 2024-T3 Aluminum Alloy," *International Journal of Fatigue*, **20**, No. 10, 737-735.
- (69) Gall, K., Horstmeyer, M.F, Degner, B.W., McDowell, D.L. and Fan, J. (2001) "On the Driving Force for Fatigue Crack Nucleation from Inclusions and Voids in a Cost A356 Aluminum Alloy," *International Journal of Fracture*, **108**, No. 3, 207-233.
- (70) Suresh, S. (2001) Fatigue of Materials, 2nd Edition, Cambridge University Press.
- (71) Davis, J.R. [Editor] (1999) Metals Handbook: Desk Edition, ASM International Handbook Committee.
- (72) Brooks, C.L., Prost-Domasky, S., and Honeycutt, K. (1998) "Corrosion is a Structural and Economic Problem: Transforming Metrics to a Life Prediction Method" *Proceedings of NATO RTO's Workshop 2 on Fatigue in the Presence of Corrosion*, Corfu, Greece.
- (73) Air Vehicles Directorate, AFRL (1999) *Corrosion Fatigue Structural Demonstration, Phase I*, AFRL-VA-WP-TR-2000-3004.

LIST OF ACRONYMS

ACAMS	Aircraft Condition Analysis and Maintenance System
AE	Acoustic emission
AHM	Aircraft Health Management (AHM)
ASIP	USAF Aircraft Structural Integrity Program
CBM	Condition-based maintenance
CCD camera	Charge Coupled Device camera
DFR	Detailed Fatigue Rating
DT	damage tolerance
ECLIPSE	Environmental Cyclic Life Interaction Prediction SoftwarE
GUI	graphical user interface
HLPM	Holistic Life Prediction Methodology
IDS	Initial Discontinuity State, AKA 'IQS'
IQS	Initial Quality State, AKA 'IDS'
MIT	Massachusetts Institute of Technology (MIT)
MRFM	Material Response Fretting Map
MRLJ	Multiple Rivet Lap Joint
MURI	Multidisciplinary University Research Initiative
NDE	Non-destructive Examination
NDI	Non-destructive Inspection
NDT	Non-destructive Testing
PSD	Power Spectral Densities
RCFM	Running Condition Fretting Map
SIF	Mode I Stress Intensity Factor
SRLJ	Single Rivet Lap Joint
WLIM	white light interference microscopy